Electronic Textiles for Motion Analysis

Joshua N. Edmison

Thesis submitted to the Faculty of the
Virginia Polytechnic Institute and State University
in partial fulfillment of the requirements for the degree of

Master of Science
in
Computer Engineering

Dr. Mark T. Jones, Chair
Dr. Thomas L. Martin
Dr. Peter M. Athanas

April 28, 2004
Blacksburg, Virginia

Keywords: Computational fabrics, e-textiles, gait analysis, context awareness

Electronic Textiles for Motion Analysis

Joshua N. Edmison

(ABSTRACT)

The union of electronics and textiles to form electronic textiles (e-textiles) provides a promising substrate upon which motion analysis applications can be developed and implemented. Familiarity with clothing allows sensors and computational elements to be naturally integrated into garments such that wearability and usability is preserved. The dynamics of the human body and the wide variety of sensor and processing choices render the typical prototype-based design methodology prohibitively difficult and expensive. Simulation of e-textile systems not only reduces these problems but allows for thorough exploration of the design space, faster design cycles, and more robust applications. Gait analysis, the measurement of various body motion parameters during walking for medical purposes, and context awareness, the recognition of user motions, are two immediate applications that e-textiles can impact and emphasize the feasibility of e-textiles as a medium for sensor deployment on the human body. This thesis presents the design of a simulation environment for wearable e-textile systems and demonstrates the use of the simulation via a prototype pair of e-textile pants.

Acknowledgements

The work presented in this thesis could not have been accomplished without the support and guidance from a variety of individuals. For those who are not mentioned specifically, thank you.

I would like to thank my advisor Dr. Mark Jones for his support, confidence, and enlightment. His advice on academics, career choices, and general life issues has been indispensable.

My thanks also go out to Dr. Tom Martin for his patience, guidance, and extensive knowledge of all things capacitive. Additionally, I would like to thank him for serving on my thesis committee.

I would also like to thank Dr. Peter Athanas for serving on my thesis committee.

I would like to thank Dana Reynolds for her tireless efforts in weaving an exceptional piece of fabric.

I would like to thank Elouise Coupey for her fabulous construction of the pants and vest garments.

Of course, my gratitude goes out all of the members of the Configurable Computing Lab and special thanks to the past and present members of the VT E-Textiles group: Zahi Nakad, David Lehn, Madhup Chandra, Tanwir Sheikh, and Ravi Shenoy.

Thanks goes to Gina for her love and support, putting up with my crazy schedule and listening when I needed it most.

Last but certainly not least, I would like to thank my parents, Jeff and Rhonda Edmison, and sister, Bridgette, for their endless support, love and interest throughout my academic career. I certainly would not have been successful without them. They are a continued source of inspiration.

This material is based upon work supported by the National Science Foundation under Grant No. CCR-0219809. Any opinions, findings and conclusions or recomendations expressed in this material are those of the author(s) and do not necessarily reflect the views of the National Science Foundation (NSF).

Contents

List of Figures

List of Tables

Chapter 1

Introduction

1.1 Motivation

As the computing paradigm is shifting from desktop machines to pervasive devices, the natural desire to bring computational devices closer to the user has been a primary goal. Achieving this goal enables a host of applications such as remote medical monitoring, interactive sports medicine, and context-aware pervasive computing that require a steady stream of information about the user's body. Familiarity and the dependence upon textiles, particularly in the form of garments, make textiles a promising deployment medium for electronic components. The advanced state of textile materials and manufacturing techniques places the computational aspects of e-textiles at the forefront of the problem domain. Early prototypes such as the Wearable Motherboard [1], shape sensing jacket [2], and piezoelectric glove [3] provided a glimpse of e-textile capabilities in wearable applications. Design rules derived and learned from the construction of a large scale acoustic beamforming array [4] showed that building e-textile systems is both feasible and beneficial. The conventional design methodology for these systems included many prototype iterations due to the large number of design variables and uncertainty about application-level algorithms. This type of design methodology is not suitable for more advanced systems. As the complexity and

sophistication of systems continues to increase, prototype-based design methodologies will become prohibitively expensive, time-consuming, and insufficient for examining the system as a whole. The primary goal of this thesis is to present and evaluate a design methodology for wearable e-textiles that utilizes simulation and a prototype that showcases this process.

1.2 Contributions

This thesis presents the design and implementation of a simulation environment for wearable e-textile systems targeted particularly towards motion analysis. The simulation environment allows the simulation of virtual sensors placed at any point on the body and can interface with application level hardware or software models. Modular design of the simulation encourages enhancement or improvement of models and applications, providing extensibility. The thesis will also show that simulation can be used not only for hardware design, but can also be used to design and test application software prior to construction of a prototype. To demonstrate this principle and verify the assertion, a prototype e-textile for gait analysis and activity context awareness was designed using the simulation. The prototype is capable of collecting data necessary for gait analysis and/or providing information about the user's activity.

1.3 Thesis organization

The thesis is organized as follows. Chapter 2 discusses background information necessary for understanding the work performed in this research. Chapter 3 discusses the details of the target applications and the design of the prototype e-textile. Chapter 4 explains the design of the simulation environment. Chapter 5 discusses the results of design space exploration using simulation and validation of the simulation via the e-textile prototype. Chapter 6 presents conclusions and summarizes the contributions of this thesis.

Chapter 2

Background

This chapter presents previous work in areas related to this research. The combined contributions discussed were utilized in the completion of the simulation environment and prototype presented in this thesis.

2.1 Electronic Textiles

Electronic textiles encompass a wide range of definitions from fabrics that incorporate conductive fibers to fabrics that contain sensors and computational devices. One of the first efforts in e-textiles, performed at MIT [5], consisted of conductive metallic organza integrated into fabric to create interactive fabrics. The first interactive fabric was a row and column-based musical keyboard. The resulting device was flexible enough to be folded and was capable of emitting the appropriate keyboard notes via external speakers. Another interesting creation was a tablecloth that identified individuals sitting at a table via RFID coasters, provided an interface via woven yes and no buttons, and included a display. Less practical applications of e-broidery were displayed via musical balls which altered their tune based on the level of physical handling, and a dress that changed color with the user's movement.

While [5] provided some interesting applications, it did not address the incorporation of other sensing and computing elements. The Wearable Motherboard project [1] marked one of the first attempts at integrating communication, processing, and sensing into a garment. Its intended application was ambulatory monitoring of soldiers in combat situations. In addition to monitoring normal vital signs the garment could detect bullet holes using optical fiber. While sensing and communication components were integrated into the textile, a computational device was worn on the hip to process data. Additional projects involving medical monitoring include the design of a garment for monitoring the major vital signs in [6], using garments incorporating metallic yarns, piezoelectric pressure sensors, and piezo-resistive threads. Respiration data was collected by using some of the sensors as strain gauges while heart data was collected using portions of stainless steel fabric. Data was collected from these sensors via an IPAQ and shipped to other devices such as a desktop PC for post-processing and analysis. The reconfigurable fabric project at UCLA [7] focused on fault tolerance and drug dispensing in an ambulatory sensing garment. The garment consisted of a token grid with interconnects that could switch the data path around a fault. The drug dispensing was performed using a non-invasive technique that administered drugs through the skin.

While the above applications showed promise, many of the e-textile design issues were not addressed. Additionally, processing elements were separated from the textile instead of being distributed and integrated throughout the fabric. The work performed by the following groups and individuals focused on many of the primary design issues and took steps towards integrating processing elements into the fabric. Modeling and simulation of power distribution/management and fabric fault/tears were investigated in [8]. This simulation allowed the investigation of power management and its effects on fault tolerance. It was shown that including power sources at finer granularities increased fault tolerance. The resulting simulation could also be used in future e-textile simulations to induce faults in the fabric. The STRETCH project [4] [9] utilized large-scale (30 foot) fabrics to deploy acoustic sensors for beamforming applications such as vehicle detection. The processing nodes were

Figure 2.1: Field test of a 30 foot acoustic beamforming textile

DSP-class processors and digital communication was performed on the fabric over wires woven into the textile. In addition to locating the direction of a vehicle, the fabric could combine data from multiple microphone arrays to calculate location. This project was also one of the first to begin integrating computational devices into the fabric. A field test of the fabric is shown in Figure 2.1. Also presented in [4] is a set of general design precepts or rules for e-textile systems. Wearable acoustic e-textiles applications, such as source separation and speech processing were explored in [10]. Specifically, the arrangement of microphones, sampling rates, and motion effects from wearing the device were investigated. These results show the importance of simulation in the design of acoustic e-textile applications and that e-textiles provide a feasible platform for acoustic applications.

The use of piezoelectric films as shape sensors in e-textiles was presented in [3]. The piezoelectric films detected the movement and tapping of the fingers in a virtual keyboard application. This work demonstrated the promise of piezoelectric films as sensing components in wearable systems due to their versatility and form factor. A photo of the prototype is shown in Figure 2.2.

Figure 2.2: Piezoelectric film-based keyboard glove

Commercial applications of e-textiles have been primarily limited to user interface methods and medical monitoring. The Burton MP3 snowboarding jacket [11] incorporates SoftSwitch [12] embroidered keypad technology. Infineon Technologies [13] produces elastic e-textile straps that weave into jackets for use with audio devices and suits which produce power using body heat. First-iteration commercial safety/medical/ambulatory monitoring devices include the LifeShirt [14] and safety sensors in furniture [15]. The Lifeshirt incorporates sensors woven into the shirt to monitor respiration, heart functions, and body orientation. Safety sensors in furniture ensure that electric recliners can only be operated by adults, will halt operation when impeded by objects, and can resize/adjust to the individual in the chair [15].

2.2 Context Awareness in Wearable Computing

The ability to place sensors near the body using e-textiles lends nicely to the requirements of context-aware systems. Context awareness as discussed in this thesis is the ability to

recognize user activity. Examples of user activity include but are not limited to walking, sitting down, standing up, running, jumping, and idle. Classification of user activity is useful for pervasive computing and health monitoring applications. Several prototype systems such as those in [16] [17] [18], attempt to fuse sensor data to form high level abstractions of the user's activity. Methods for achieving activity awareness include the use of neural networks, decision trees, Markov chains, probabilistic models, and state machines. The work performed by Golding *et. al.* [17] focused on the use of several sensor types (accelerometer, magenetometer, light, and temperature) to determine the activity and room location of the user. In doing so they discovered the importance of pre-processing sensors data prior to classification. Application of learning algorithms, specifically Markov chains, to data that was not pre-processed typically led to greater error.

Van Laerhoven *et. al.* [16] used several different sensor types including accelerometers and light sensors that were attached to a circuit board that was small enough to wear. Kohenen Self-Organizing maps were utilized as the learning/classification algorithm. A push button interface was provided that allowed the user to train the system to recognize a various task or activity. Recognition accuracy ranged from 42%-96%. Randell *et. al.* [18] also investigated the use of clustering neural network algorithms for determining user context. Their work examined the validity of using a single accelerometer and minimizing power by using a very low sampling rate. Quoted accuracy for several motions average roughly 75%. Later work by Van Laerhoven [19] incorporated a relatively large number of sensors, more than thirty, the majority of which were accelerometers, to determine user activity. The resulting device was a harness-like system that was worn on-top of existing clothing. Accelerometers and computational devices were attached to the harness at various points of interest. The system demonstrated distributed processing of the Kohenen learning algorithms introduced in earlier works [16]. Work was also performed using sensors such as microphones and cameras. Clarkson *et. al.* [20] attempted to extract context features, particularly movement through a building, from sound and video data. The classification mechanism used hidden Markov models that were trained offline. The hidden Markov models were trained over a

variety of observation windows and number of classification states to find an optimal model. Farringdon *et. al.* [2] developed a badge and jacket that could determine the user's context. Additionally, the idea of sensing the shape of the body was introduced. This was achieved by using metallic woven strips whose resistance increased as they stretched with user movement. The algorithm used to extract context consisted of basic decision-tree style criteria such as thresholds and boundary crossings.

2.3 Biomechanics and Gait Analysis

Because of their close coupling to the human body, another interesting application area for e-textiles is biomechanics. Biomechanics is loosely defined as the study and analysis of mechanical behavior of living organisms, typically humans [21]. Common areas of applied biomechanics are ergonomics, gait/locomotion, motor control/muscle, orthopedics, and sports medicine/performance [22]. Biomechanics in ergonomics focuses on the design of systems and spaces that operate well with the human body (i.e. are comfortable and do not cause harm). Commercial companies such as Insight [23] and academic groups such as Kinetics Laboratory of Ottawa [24] and the Virginia Tech Locomotion Research Lab [25] utilize biomechanics to reduce injury and fatigue in the workplace or caused by products. An example application, the design of car controls to reduce driver hazard, is under investigation at the Virgina Tech Locomotion Research Lab [25]. Motor control and muscle strength are also two well examined functions of biomechanics, particularly in rehabilitation efforts. Combining the computer and exercise equipment to form devices similar to Cybex machines [26] allows doctors and medical technicians to observe status and progress in graphical representations of force curves, moments, and other appropriate readings. Comparison to known ideals for various age groups and long-term historical tracking are also helpful in enhancing treatment.

Biomechanical analysis is also used for improving sports performance. The use of motion

capture systems to capture golf swings, running motions, throwing motions, and other sports related movements may pinpoint incorrect movements or variations that more subjective analysis cannot [22]. In addition to sports performance the same techniques may be applied to injury prevention or evaluation of sports devices, such as shoes and racquets.

Current studies in gait analysis investigate the slips and falls in elderly and their associated causes. Work performed in [27] examines how elderly individuals react to slippery surfaces and how age affects these reactions. Additional studies include the investigation of muscle strength effects on slips and falls [28], aging effects on slips and falls, development of a hip airbag, and how carrying loads effects slips and falls. Gait analysis is also a strong indicator of various medical conditions such as Parkinson's Disease and undetected strokes [29]. Current systems for performing these analyses consist of camera-based motion capture systems [25]. These systems provide three-dimensional position data that can be used to calculate necessary parameters. Typically calculated parameters are: step length, heel strike velocity, slip distance, slip velocity, required coefficient of friction, and center of mass.

2.4 Simulation Using Ptolemy

The Ptolemy II simulation environment allows concurrent simulation and interaction of different models of computation [30]. In doing so, Ptolemy II requires the user to divide the design into models of computation and implement these models within Ptolemy II actors. Actors provide process encapsulation and hierarchy such that they can be easily manipulated and connected in the Ptolemy II data flow processing method. The actions of the actors are controlled not only by the design implementation but also by the computational domain in which they exist. Actors are connected together to complete the simulation. The primary models of computation supported are: Discrete Event, Finite State Machine, Synchronous Dataflow, Process Network, and Continuous Time. E-textile systems require the continuous time domain, discrete event, and finite state machines domains. Sensors that interface with

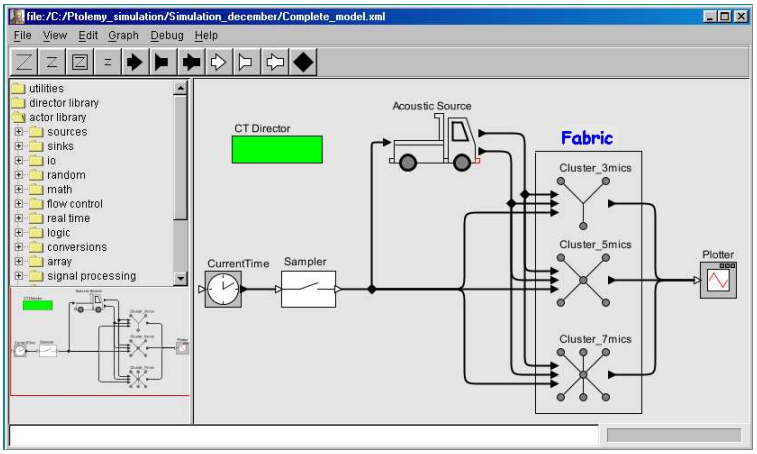

Figure 2.3: A general view of the Ptolemy II simulation environment

the analog, real-world are modeled in the continuous time domain and must interface with the Discrete Event domain. The Discrete Event and Finite State Machine domains model microcontrollers and other processing elements. Communication between sensors and processing elements is implicitly performed using the data flow processing model enforced by the Ptolemy II framework. A screenshot of a typical Ptolemy II development and simulation environment is shown in Figure 2.3.

Chapter 3

Applications

To create meaningful and successful simulations, the target applications and how they relate to the implementation platform must be fully understood. The close coupling of textiles, and consequently, e-textiles to the human body, lends naturally to motion analysis. Motion analysis applications can be loosely subdivided into to two primary categories, telemetric and inferential. Telemetric applications typically consist of basic sensor data collection while inferential applications attempt to glean highly abstracted information from sensor data. Two applications, one from each category, were chosen as targets: motion context awareness and gait analysis. This chapter discusses the applications and associated design issues. Chapter 4 will discuss the use of simulation to resolve design variables and Chapter 5 will discuss the details of the implementation and associated results.

3.1 Context Awareness

Context awareness is the ability of a device to derive the user's activity, the user's location, the user's company, or what resources the user is near. This type of information allows the device to better interact with the user and the user's environment. For example, a context-

aware cell phone that knew its location would not ring while you were sitting in a movie theater or while you were in a meeting. Context awareness systems can be physically based like the cell phone, or can be non-physical such as a context-aware help menu in a word processor. For the purpose of this thesis, context awareness will refer to the recognition of human motions, for example, walking and running. Practical applications of context awareness in this form include fall detection/prevention in elderly patients, health monitoring, and ubiquitous computing.

3.1.1 Problem Statement

Recognizing user motions is not a new concept [20], but has been hampered by the difficulty of placing sensors near the body discretely and comfortably. Also difficult, is the mapping from low-level sensor data to higher level abstractions [16]. Machine learning algorithms for fusing low-level sensor data such as neural networks or statistics-based algorithms tend to require relatively large amounts of storage, processing power, and may be trained prior to use [31]. Due to the complexity of these algorithms, changing design variables often produces unpredictable or non-intuitive results, further complicating the design process. Implementation of context-aware systems involves the consideration of many variables. To successfully design context-aware systems these variables must be understood.

3.1.2 Design Variables

All context-aware systems in the physical domain involve the use of sensors. Sensors, by definition, provide the interface between the physical world and computational resources. The first design variable is the type of sensors. Selected sensor types must be capable of capturing information which is fundamental and differential to the types of motions or activities that are to be recognized. The underlying physics of the motions and activities usually determines what type of information is fundamental, but the task of differentiation is

typically left to the algorithms. Popular sensor choices in past examples of context awareness [2] [16] [18] have been accelerometers, gyroscopes, compasses, light sensors, and other devices capable of sensing spatial or environmental conditions.

The number of sensors used is also a variable in the design. Using too few sensors results in incomplete or insufficient information, while too many sensors results in data saturation and over constraint of the recognition algorithms. This problem is compounded by the fact that raw sensor data may be pre-processed into multiple representations such as averages or standard deviations causing data saturation with fewer sensors. Increasing the number of sensors may also provide rudimentary fault tolerance, reducing the effects of sensor loss.

Sensor quantity is tightly correlated with the placement of sensors. Sensor placement, at the very least, provides a lower bound on the minimum quantity of sensors. Also, sensor placement dictates the *level* and *quality* of access to the fundamental physical information. Proper selection of sensor types can be negated by poor sensor placement choices. When considering sensor placement for context-aware systems that intend to discern motion and activity information, one must compensate for the large variations in degrees of freedom of different body parts. Primary sensor locations may require placement of additional secondary sensors in the vicinity to correct for and resolve degrees of freedom. For context awareness applications, algorithms may be capable of recognizing context even with partially incorrect data.

The core of most context-aware systems are the algorithms that generate the context information. Proper selection of parameters for these algorithms is paramount to the success of context-aware systems. Selection of these parameters is discussed in Section 4.6.1. Machine learning algorithms such as neural networks, statistics, and decision trees provide methods for fusing low-level sensor data and making highly abstracted inferences. Within the neural network sub-class of learning algorithms are many specific types of neural networks such as backpropagation, recurrent, probabilistic, and clustering [32]. When the algorithm for differentiating inputs is not known or is extremely difficult to derive, neural networks, if properly

configured and trained, can provide a hands-off, black-box solution. Neural networks also have the ability to recognize highly dimensional data, lending well to the requirements of context awareness applications.

While this may sound ideal, neural networks have several drawbacks and a large number of design variables. The user of a neural network must choose the type of neural network, the number of layers, the type of output, the number of inputs, the layer functions, and the pre/post processing algorithms. Finding the sweet spot in this design space is a daunting challenge. When choosing these variables, the available computation resources and data storage capabilities must be considered. Prior use of neural networks for activity recognition [17] showed that raw sensor input is not suitable and should be pre-processed preceding presentation to the neural network. The choices for pre-processing algorithms ranges from averages to complex statistical functions. Post-processing of neural network output using state machines or Markov chains can eliminate unlikely or impossible activity state transitions, increasing accuracy beyond that of raw neural network output [16]. For example, it would be impossible to stand up if you are already standing. For the purpose of this thesis, neural networks will be the exclusive machine learning algorithm used. It is important to note that this selection, based upon previous work discussed in Chapter 2, was necessary to limit scope.

Implementing context awareness using a wearable e-textile garment poses additional design considerations. Similar to all wearable systems, e-textiles are subject to the same dynamic environment. As discussed previously, sensor placement is critical to application success. The range of sizes and shapes across the human population is quite large. As a result, an e-textile with one size may experience variations in sensor placement, with respect to locations on the body, over a large population. Clearly, multiple garment sizes will be required. To stay within the confines of standard textile manufacturing processes, the minimum number of garment sizes required to reduce sensor placement variations must be found. In addition to placement variations, the dynamic range of the sensors across the population must also be considered. An example of variations in dynamic range is larger acceleration

values for those individuals who have longer legs. Further sensor variation may result from sensors being embedded within the textile, making them susceptible to error caused by cloth motion. Dynamic environments increase the chance of sensor failure, raising the need for fault tolerance in the system and or algorithms used to determine context. The effects of sensor placements on the context awareness application discussed in Section 5.2.

3.1.3 Design Goals

The design goals for a wearable, context-aware, e-textile are:

- **Accuracy:** The e-textile must be capable of providing an application specified accuracy.
- **Generalization:** The e-textile should be able to generalize across a broad range of populations and situations.
- **Fault Tolerance:** The e-textile should be able to provide the necessary level of accuracy given the loss of some subset of sensors.

Clearly, when considering all of the primary and secondary design issues of context-aware systems the result is a combinatorial explosion of options. This makes fully exploring the design space very difficult, if not impossible. Later, it will be shown that simulation is a useful tool for thoroughly exploring the context awareness design space.

3.2 Gait Analysis

The second promising application for wearable e-textiles is the monitoring and measurement of the human walking motion, known as gait analysis. Of particular interest are various characteristics of the walking motions that may provide causes for certain medical conditions.

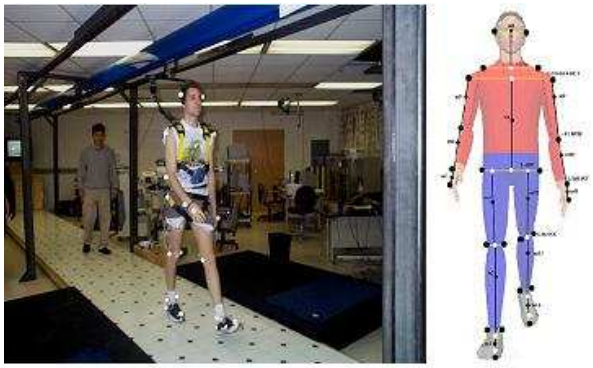

Figure 3.1: Subject outfitted with retroreflectors in the Virginia Tech Locomotion Laboratory (used with permission from Thurman Lockhart, Virginia Tech Locomotion Laboratory)

Examples of this include investigating how and why elderly people fall, and effects of aging on the walking motion [25].

3.2.1 Problem Statement

Current gait analysis techniques involve costly equipment consisting of cameras and retroreflective markers that are capable of providing three-dimensional position information of the limbs and torso. The test subject is outfitted with the retroreflectors, shown in Figure 3.1 [25], such that they are placed at points of interest and are recorded performing some action using six cameras. Captured video is post-processed using proprietary software to extract the three-dimensional motion data. The final result is XYZ coordinate information corresponding to the positions of the retroreflectors. In addition to the three-dimensional motion data, force plates embedded into the walking platform record forces on the feet during motion. This combination of data is used to calculate a set of dependent parameters required to perform the analysis.

E-Textiles provide a probable alternative to this method. While e-textiles cannot provide three dimensional position information, they can be used to directly observe the required dependent parameters. Additionally, an e-textile implementation of a gait analysis system would be relatively less expensive and portable, allowing the investigator to collect data from the subject in a more natural setting such as a home or office or allow data collection over a longer period of time. Similar to the context awareness application, a variety of design variables exist for the successful design a wearable, e-textile, gait analysis system.

3.2.2 Design Variables

Gait analysis is subject to all of the sensor related design variables discussed in Section 3.1. The placement of the sensors, number of sensors, and type of sensors will ultimately determine how well the desired information is extracted from the physical situation. There are however several distinct differences between the design considerations for the two applications.

Gait analysis requires a different type of accuracy than the context awareness application. Context awareness requires that the mapping to higher level abstractions is accurate and suggests that the context algorithms should be tolerant of sensor data variations. Gait analysis, however, is directly dependent upon the sensor data. The lower bound of the accuracy depends heavily upon the type of gait analysis desired. Accuracy is affected by a number of different items such as the sensor technology available, interface circuitry, garment construction, sensor placement, and degrees of freedom. How these variables contribute to the overall deviation varies given a particular type of analysis.

The dynamic range of sensors is also important in a gait analysis application because of the reliance upon the raw sensor data. Improper configuration of the sensing range may result in clipping or reduce the sensor data below the noise thresholds. These types of errors could cause significant error in the calculation of dependent measures. The variation in sensor output across the body is quite large. For example, an accelerometer placed on

the heel produces accelerations orders of magnitudes larger than those of an accelerometer placed on the hip.

Again, due to the necessity of accurate sensor data, sensor degree of freedom is a crucial design variable. A high degree of freedom may force a sensor to change orientation and cause errant sensor readings. Other sensors may be required to provide information for detection and correction of changes in sensor orientation. Body parts whose possible motions have a high degree of freedom such as the ankles, heels, elbows, and wrists are the most difficult to sense. Some types of sensors are generally not affected by additional degrees of freedom such as the piezoelectric films and microphones.

3.2.3 Dependent Measures

To fully perform the same gait analysis applications enabled by video motion capture technology, the e-textile must be capable of measuring the appropriate set of dependent measures. These measures are listed with descriptions below [28]:

- **Step Length:** The distance traveled by the foot between alternate foot heel strikes.
- **Sliding Heel Velocity:** The horizontal velocity of a heel during the slip initiation phase.
- **Slip Distance:** The horizontal distance traveled by the foot that initiates the slip.
- **Heel Velocity:** The heel velocity during the heel strike.
- **Required Coefficient of Friction:** The ratio between horizontal and vertical forces on the foot.

While there is some overlap in the design variables for the context awareness and gait analysis applications, each exhibits unique requirements. It is expected that most conceivable applications of wearable electronic textiles will have general, sensor-related design variables

coupled with a subset of unique requirements. With the design variables in mind, the prototype e-textile platform will be discussed in Section 3.3. Details involving the utilization of the prototype platform to implement the context awareness and gait analysis applications will be discussed in Chapters 4 and 5.

3.3 Prototype Construction

The e-textile platform chosen to implement the desired applications is a pair of pants. Pants allow sensors to be placed on the legs, feet, and near the center of mass. These qualities fit nicely with the gait analysis and context awareness applications. The e-textile also incorporates the precepts presented in [4] such as generalized fabric swatches to maintain large scale manufacturing capability, digital communication across the textile network, small-scale sensor nodes, and mechanical attachment.

3.3.1 Design Assumptions

For both applications, two fundamental pieces of information must be sensed, specifically, physics of motion and shape of the body. All of the physical measurements such as velocity and position can be derived from acceleration, thus accelerometers were selected as a sensor type. Prior work performed in [3] demonstrated the feasibility of using piezoelectric films to detect shape. Consequently, piezoelectric films were chosen for sensing the shape of the body. While other sensors choices may be justifiable, piezoelectric films and accelerometers will comprise the full set of sensors investigated in this thesis.

Two important aspects of an e-textile for wearable applications are that it must be comfortable to wear, and sensors must be integrated with minimal obtrusiveness. The cloth for the pants was created using a manual weaving process with a thread pitch of approximately twenty-four threads per square inch. The use of a generalized fabric swatch incorporating

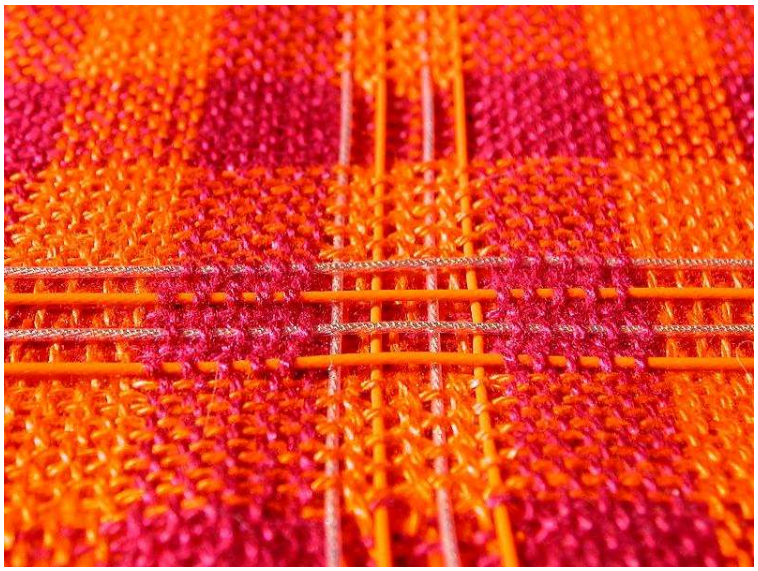

Figure 3.2: Physical implementation of the generalized fabric swatch

the insulated bus wires for communication shown in Figure 3.2 enabled the manufacturing of large cords of fabric. The cords of fabric were cut and sewn into the final pair of pants. Connections between the fabric and sensor nodes were made using insulation displacement connectors created using off-the-shelf components shown in Figure 3.3 [33]. The connectors were designed with a minimal profile in mind. While these connectors are not the optimal solution, they were satisfactory for a first iteration prototype.

The computational architecture of the pants was constructed in a hierarchical fashion. The bottom-most layer of the hierarchy consists of lightweight sensor nodes that utilize eight-bit PIC16LF18 [34] microcontrollers running at 8MHz to provide analog to digital conversion and simple pre-processing of data. Pre-processing was performed at the sensor node to reduce the amount of required network traffic. The next layer in the hierarchy consisted of a single master node consisting of larger Atmel AVR [35] microcontrollers running at 20Mhz and a RS232 port which queried, via interrupts, the smaller sensor nodes for their data. Communication between the two lower layer of sensor nodes was performed on a shared I^2C [35] bus created using the generalized fabric network. The collected sensor data was forwarded via the RS232 interface to a 200MHz IPAQ, which relayed the data to a desktop

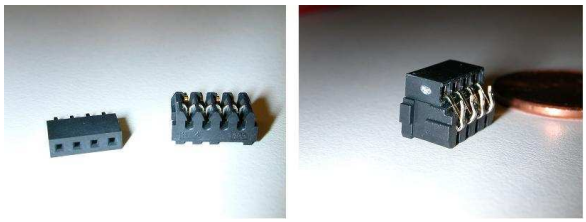

Figure 3.3: Off-the-shelf components used to construct the connector and the finished product

computer for processing and analysis as shown in Figure 3.4. Other nodes required were an ON/OFF power node, and an I^2C bus terminator. The bus architecture consisted of four wires: power, ground, clock, and data. The clock and data lines were required for the I^2C bus. Power for the entire e-textile was provided by a 9 volt battery.

The accelerometer sensor nodes utilized the ADXL311 dual-axis accelerometer [36]. The ADXL311 was chosen for a low operating voltage, analog output, small package, and low g resolution capabilities. To provide minimal noise and maximum resolution the accelerometer was configured with a 1Hz bandwidth. The low operating bandwidth was justified by the low frequency of human motion. Analog output was converted to the digital domain using the 10-bit onboard PIC analog to digital converter (A/D). The accelerometer was operated at 3.3V and the A/D was provided with upper and lower reference voltages of 2.2V and 1.1V, respectively. These voltages were selected to fit the dynamic range of the sensor. Note that the radiometric operation of the accelerometer provided a zero-g bias voltage of $\frac{V_{DD}}{2}$ or 1.65V.

The piezoelectric film sensor nodes utilized the 6" DTK052 laminated, piezoelectric film from Measurement Specialties, Incorporated [37]. This particular film was chosen for length, lamination, and riveted wires. The 6" length of the film allowed for use in sensing joint angles and was most forgiving in placement. Analog interface circuitry consisted of a voltage divider that provided a bias voltage. Biased piezoelectric output was routed through an operational amplifier to satisfy input impedance requirements and then into the A/D. Analog output

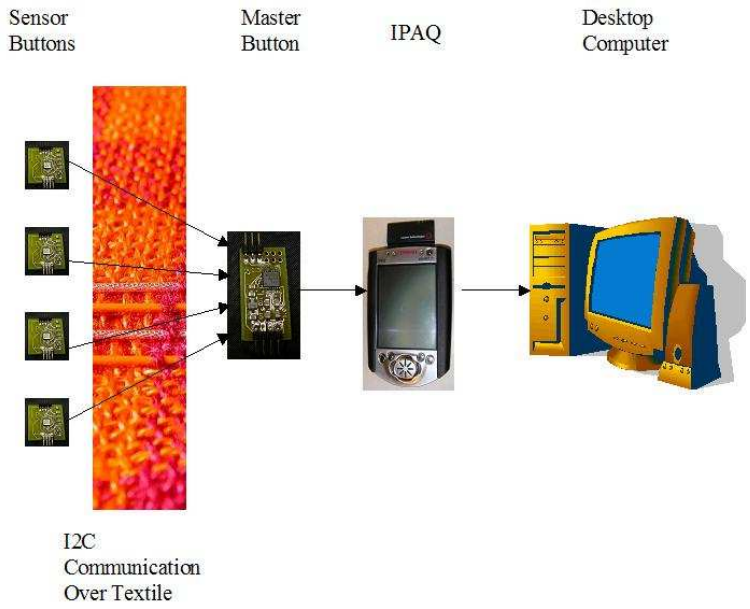

Figure 3.4: Pants architecture block diagram

was converted to the digital domain using the 10-bit onboard A/D. The piezoelectric sensor itself does not require power, but the corresponding interface circuitry was operated at 3.3V and the A/D was provided upper and lower reference voltages of 3.3V and 0V, respectively. Similar to the accelerometer button, the A/D reference voltages were selected to best fit the dynamic range of the sensor.

The operating voltage for all components on the textile was 3.3V. The power provided by the 9V battery was distributed throughout the fabric via the power line on the bus. The 9V source voltage was reduced to 3.3V at each sensor node by a power regulator. This provided the capability to accommodate sensor or computational nodes with different operating voltages.

The master implementation, aside from the previously mentioned hardware features, consisted of a simple routine which queried the sensor nodes identified by their I^2C addresses and sent the data across the RS232 port. If further processing had been desired the master button could have provided the necessary computational power, however this was not re-

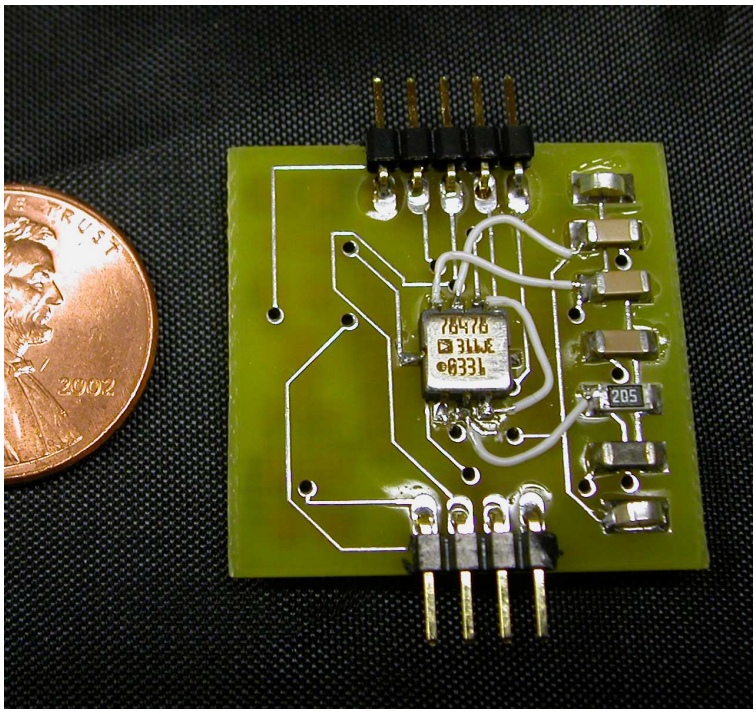

Figure 3.5: Physical implementation of an accelerometer button

quired. Development of the software for Atmel device on the master button was performed using a C cross-compiler.

The software architecture of the sensor nodes was developed in low-level PIC assembly. Higher level languages such as C were not used for the smaller PIC devices due to a lack of available compilers. The basic algorithm implemented performed the following cycle of operations: sample A/D, store the value, pre-process (if necessary), send data if an interrupt is received. For ease of use, the algorithms were written generally, such that the same routine could be used on all sensor nodes. Some features such as software selectable channels, pre-processing window size, and sampling rate were included for easy modification and application switching. Efficient computation of pre-processing algorithms was achieved by retaining a circular buffer of values sized to the requested pre-processing window size and storing intermediate calculations. This allowed subsequent calculations to perform a single subtraction of the oldest value and addition of the newest value instead of summing the

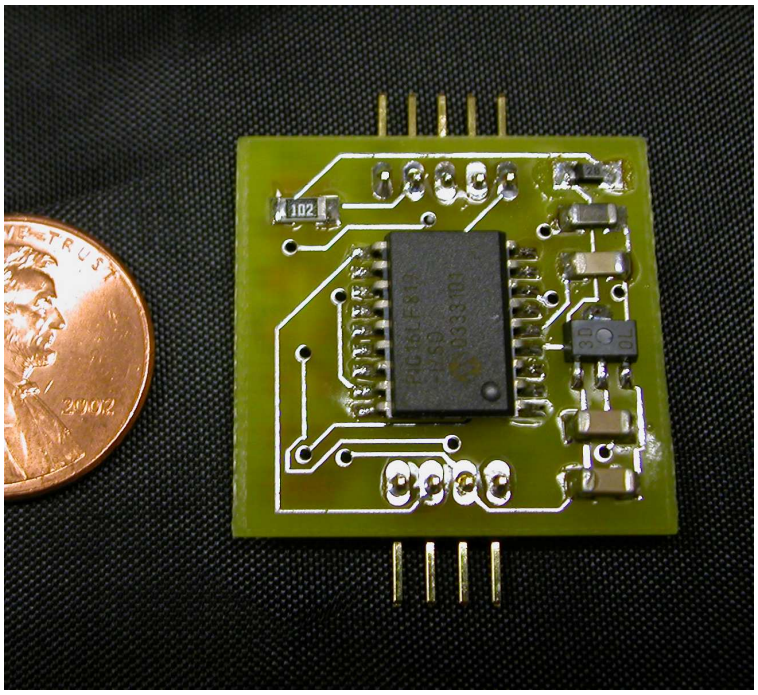

Figure 3.6: Physical implementation of a piezoelectric film interface button

entire set on every iteration. Double buffering of the data was required to ensure valid data was sent when interrupted during pre-processing routines. Each node, upon programming the memory with the routine bitstream, required the assignment of unique identification number for use as an I^2C address. This value was loaded into the first location in EEPROM. A photo of the finished pair of e-textile pants is shown in Figure 3.8 and Figure 3.9 .

With a set of applications and a platform for evaluating various configurations and selection of design variables, Chapter 4 will explore the design space via simulation of the sensors, physical environment, and applications.

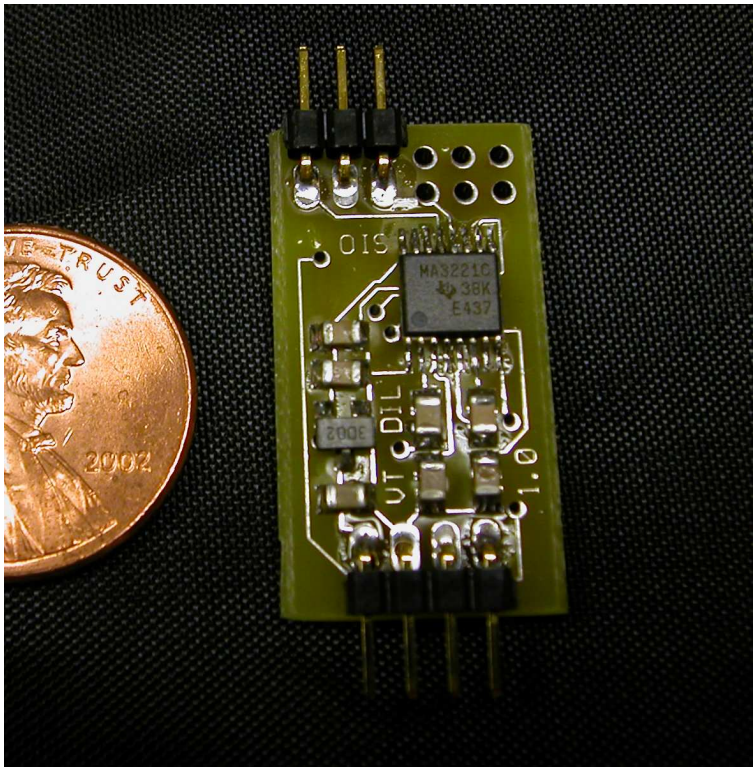

Figure 3.7: Physical implementation of the master button

Figure 3.8: Finished e-textile pants prototype (shown inside-out)

Figure 3.9: Prototype pants worn by Josh Edmison (with matching vest)

Chapter 4

Simulation Environment

Because of the large design space of wearable sensor networks in e-textiles, simulation is the only realistic method for thoroughly exploring the design space. While a full simulation of an e-textile system would be ideal, such as that performed in [4], which includes the physical fabric, fault tolerant networking, and power, it is unnecessary for investigating many of the design decisions and is beyond the scope of this thesis. A minimal simulation environment for wearable, e-textile applications must include sensor models, driving sources for the sensor models, and methods for implementing application specific processing. The simulation environment presented contains the necessary features for accurately modeling the applications and traversal of the design space.

4.1 Methodology

The foundation for the simulation implementation was the Ptolemy II [30] simulation environment. Ptolemy II was selected because it allows simulation across multiple models of computation such as finite state machines, data flow, discrete event, and continuous domains. Additionally, Ptolemy II is open-source, free, and is the basis for the TailorMade [38] simula-

tion environment. The developed simulation must allow integration with the interrupt-driven model of computation developed in [4] such that future work could encompass the simulation of the entire textile and its applications. Due to the complexity of application level algorithms and a desire to provide flexibility, the application level algorithms were implemented using MATLAB and will be discussed in later sections. The design of the simulation platform consisted of four major phases: sensor model development, sensor model validation, application model development, and application model validation.

4.2 Simulation Benefits

Simulation offers many benefits over iterative prototype development solutions. Among these benefits are lower cost, fewer design iterations, repeatability, testing over a larger population, no need for human subjects, and speed. Prototypes are almost always expensive, difficult to construct, and prone to faults due to the learning curve. Simulation eliminates the need for prototypes during the application design phase and is subject only to developer induced faults. The cost of simulation is low, assuming the existence of reasonable simulation frameworks and adequate technical skills required to manipulate the software.

Aside from the obvious cost and time benefits, simulation offers some unique properties that cannot be achieved using conventional prototype-based development cycles. The first of these attributes is repeatability. Having mathematical sensor models and known data for driving sensors allows the designer to *exactly* repeat experiments, assuming that there are no non-deterministic elements of the system such as randomly generated input. This is particularly useful when examining anomalous or counter-intuitive results. Another attribute of simulation not found in prototypes is the ability to easily and quickly test or train the device over a large population and/or scenarios. Given appropriate data sets, a simulation environment can produce results at speeds limited only by the speed of the execution platform. Training a prototype over the same population or scenarios would require

far more manpower to setup the device and the difficulty that is associated with managing human test subjects. Eliminating the need for human subjects greatly reduces the logistical complexities. Because of the increasing complexity of e-textile systems and their enormous design space, simulation is not just a luxury, it is a necessity. The benefits of simulation help achieve quality designs in a reasonable amount of time and money.

4.3 Human Motion Data

To drive the sensors and perform useful simulations, a realistic data source for human motion must be used. The source selected was human motion capture data. Human motion capture data is the three-dimensional XYZ position data for various points on the body obtained from the videotaped subjects discussed in Section 3.2.1. An example visualization of human motion capture data is shown in Figure 4.1. The Human Motion Capture Database project at CMU [39] contains a large collection of data sets and corresponding that which are freely available. The file format of the data sets was the .c3d file format which is used extensively for motion capture data [40]. The sampling rate of the data was 120Hz.

Initial inspection of the motion data for the purpose of driving sensors resulted in a significant problem. When acceleration was calculated from the data using the equation discussed in Section 4.4, there was a large amount of high frequency noise as shown in Figure 4.2. To correct for the high frequency noise, it was necessary smooth the data using the MATLAB spline toolbox. Previous work performed in [41] discusses the smoothing of motion data using a 4th order Butterworth filter. Research into the accuracy of the camera and retroreflector based motion capture systems revealed that the maximum resolution was approximately 2-4mm. The data was splined to this level of tolerance and the problem was corrected. The splined data is shown in Figure 4.2.

The high frequency noise problem also affected the calculations for the piezoelectric film sensor model, but the spline-based process also corrected this problem. Unfortunately, the

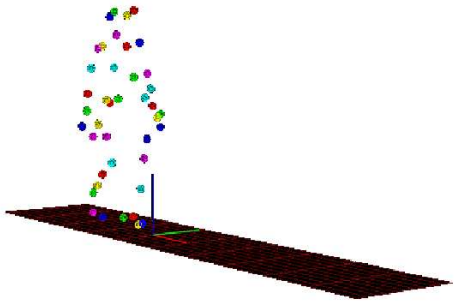

Figure 4.1: Motion capture data visualization

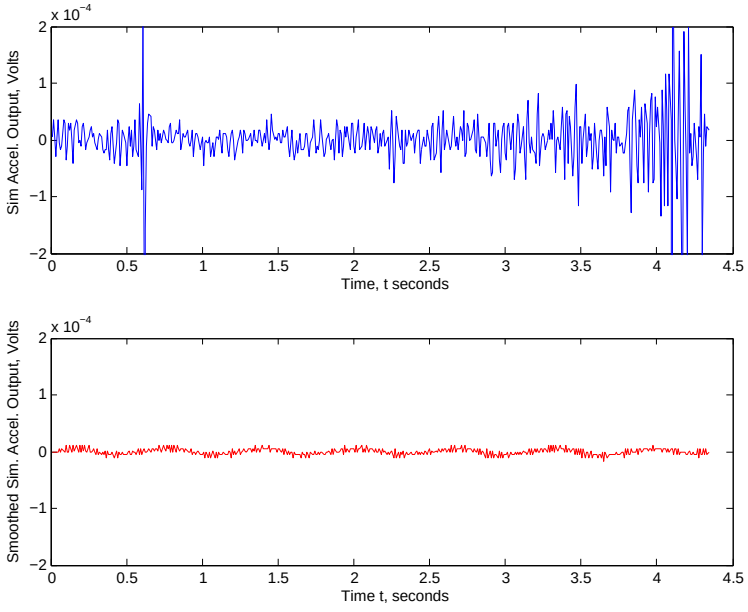

Figure 4.2: Result of smoothing the human motion capture source data

motion capture files lacked the force plate data, discussed in Section 3.2.1, necessary for modeling piezoelectric film sensors as force sensors.

4.4 Accelerometer Sensor Model

The accelerometer simulation model was based upon the operational characteristics of the Analog Devices ADXL311 dual-axis accelerometer. The model calculates acceleration along the appropriate axis given three, three-dimensional position points (x_1,y_1,z_1,),(x_2,y_2,z_2,),(x_3,y_3,z_3,) and a known and constant sampling rate F_s. The approximation for each acceleration point where $\Delta t = \frac{1}{F_s}$ is $\frac{(x_1 - 2*x_2 + x_3)}{(\Delta t^2)}$. A sliding window of size three is used on a discrete data stream and each acceleration value is calculated. The resulting values are converted to m/s^2 and then to g's, which will be referred to as acc using the Earth's gravitational constant of 9.81 m/s^2. The resolution attribute of the ADXL311 specifies an output voltage of $Vout = ((V_{DD}/5.0) * 315mV * acc) + \frac{V_{DD}}{2}$. Substituting the operating voltage of the accelerometer sensor node on the prototype, the equation for $Vout$ becomes $Vout = (206mV * acc) + 1.65$. Using this result, the acceleration values in g's are converted to the output voltage. The option also exists to further convert the voltage values to A/D readings if the sensor is to be used in an interrupt driven computational model such as that in [4].

To ensure a correct model and proceed to the next phases of the accelerometer sensor design, the model needed to be validated. The platform chosen to validate the mathematical accelerometer model was a simple pendulum, shown in Figure 4.4. When the second order differential equation describing the angle θ as a function of time is solved, the resulting analytical solution for the pendulum angle is $\theta(t) = \theta_{MAX} * sin(\sqrt[2]{\frac{g}{L}} * t)$ [42]. From this equation the x and y position functions can be derived, $x = L*sin(\theta)$ and $y = L*(1-cos(\theta))$, where $\theta = \theta(t)$ evaluated at time t. Taking the second derivative of the x and y position equations and the first derivative of $\theta(t)$ yields the x and y time-dependent acceleration

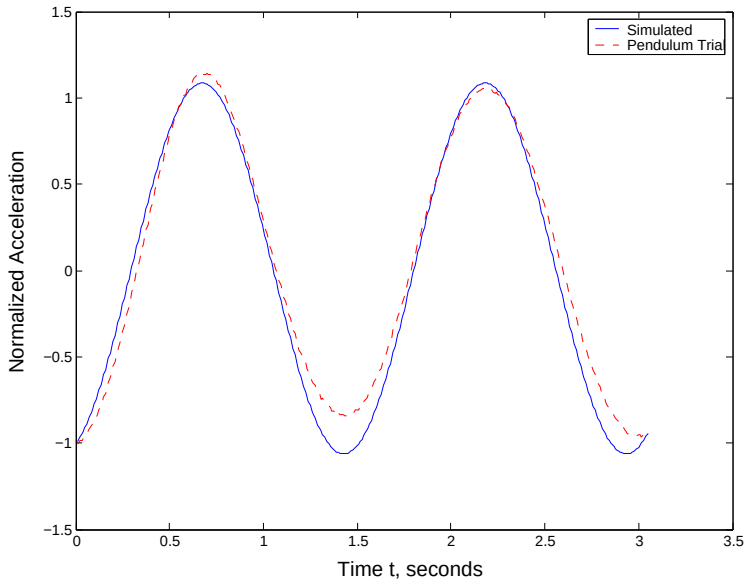

Figure 4.3: Verification of mathematical accelerometer model using a pendulum

equations $x'' = -L * \theta(t)'^2 * sin(\theta)$ and $y'' = L * \theta(t)'^2 * cos(\theta)$. Validation consisted of placing the accelerometer on the head of a simple pendulum such that the accelerometer would measure the acceleration along the x-axis. To minimize the change in orientation of the sensor, the maximum initial angle was no greater than 15°. Data was collected from the accelerometer during a pendulum swing and the results were compared to the derived analytical equations as shown in Figure 4.3.

The results confirmed that the accelerometer model was accurate. The slight deviations are likely a result of the orientation change caused by the pendulum swing. While it was not necessary to correct for orientation change for the validation of the mathematical model, it was necessary to accurately model the accelerometer in certain placement situations that cause the accelerometer axis to change orientation in three-space. An example of this situation is the placement of an accelerometer on the heel, oriented such that accelerations in the horizontal and vertical directions are measured.

During the lower leg swing-back phase of the stepping motion, the heel and foot structure changes orientation such that the foot is no longer parallel with the ground. This causes

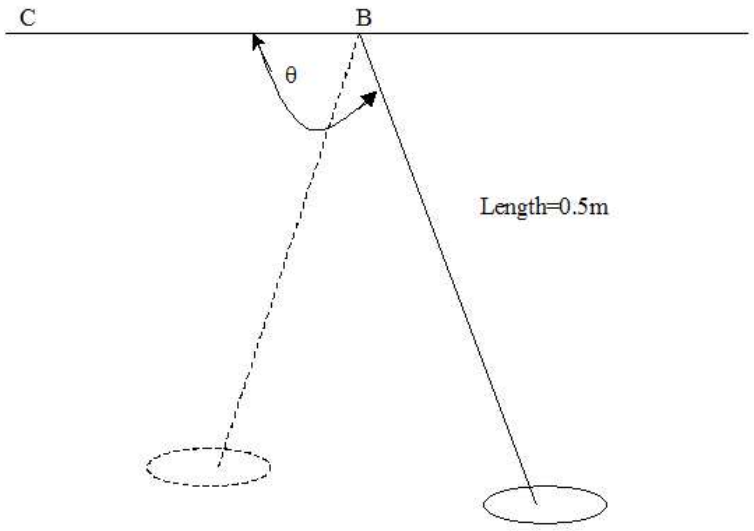

Figure 4.4: Drawing of pendulum setup used for verification

the x axis of the accelerometer to partially sense acceleration in the z direction and vice versa. In the basic accelerometer model discussed previously, this is not considered. The accelerometer can be extended to accommodate a heel-type scenario by requiring three more XYZ triples that can be manipulated to resolve the amount of orientation change. This information can then be used in conjunction with a rotation matrix to produce the correct output. The rotation matrix is governed by the equations $Xnew = x * cos(\theta) + y * sin(\theta)$ and $Ynew = y * cos(\theta) + x * sin(\theta)$, where θ is the amount of rotation in degrees from the original orientation.

To provide maximum simulation flexibility a method must be available to enable placement of the sensors on any point of the body. Because the human motion data used to drive the simulations consists of three-dimensional coordinates, enough information exists to generate the position coordinates for any point on the body. This is limited to the specific points on the body that were recorded during the motion capture session. The translation algorithm requires two XYZ coordinate sets, a source and destination, (x_1,y_1,z_1,),(x_2,y_2,z_2,) and a translation distance δd. The algorithm produces new XYZ coordinates for a virtual point δd units from the destination coordinates. To perform the translation the Eu-

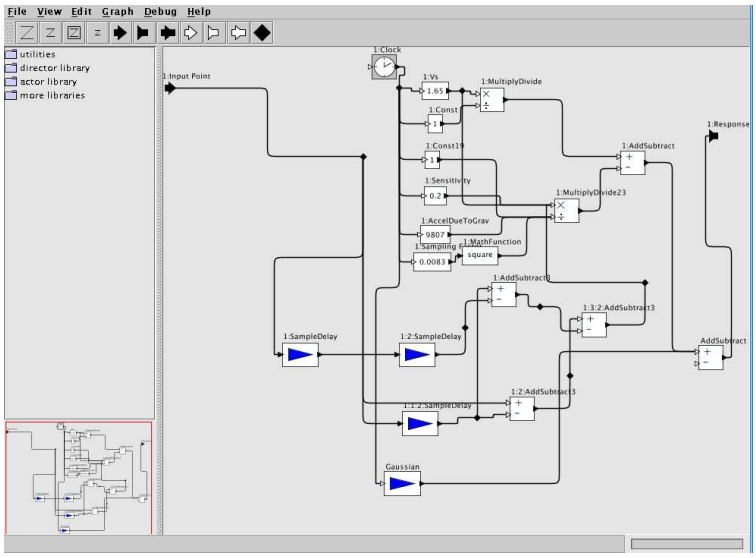

Figure 4.5: Ptolemy II model for a single accelerometer axis

clidean distance between the source and destination must be calculated using the equation $dist = \sqrt[2]{(x_1 - x_2)^2 + (y_1 - y_2)^2 + (z_1 - z_2)^2}$. The vector created by the source and destination coordinates is $\vec{V} = (x_2 - x_1)v + (y_2 - y_1)w + (z_2 - z_1)f$. The unit vector $\vec{V}_{unit}$ is obtained by $\vec{V}_{unit} = \frac{\vec{V}_{unit}}{dist}$ and is in the same direction as the line created by the two XYZ triples. The distance from the source point to the new virtual point $dist_{new}$ is found by $dist_{new} = dist - \delta d$. The new destination point is found by multiplying the unit vector by $dist_{new}$, $\vec{V}_{new} = \vec{V}_{unit} * dist_{new}$. Finally, to anchor the vector to its original spot, the original source point is added to $\vec{V}_{new}$. The result of this operation is an XYZ triple corresponding to the position of the virtual point. This operation can be performed between any two points. The use of this method in design exploration will be demonstrated in Section 5.2. The finalized Ptolemy II accelerometer sensor model is shown in Figure 4.7.

4.5 Piezoelectric Film Sensor Model

The model of the piezoelectric film was based upon the operational characteristics of the Measurement Specialties DTK052 piezoelectric film sensor [37]. Piezoelectric film sensors

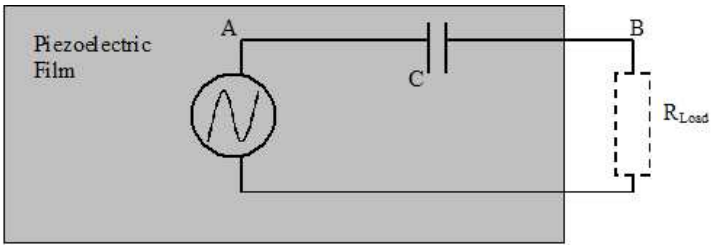

Figure 4.6: Equivalent circuit for piezoelectric film

were included in the selected sensor set for sensing the shape of the body and force measurements. To correctly model the operation of the film, its underlying operation must be understood. Piezoelectric films do not require power to operate and when stimulated physically produce voltage. The equivalent circuit of the film consists of an ideal, strain-dependent AC voltage source in series with a capacitor [37] similar to that shown in Figure 4.6. While it is not possible to access the node denoted by letter A in Figure 4.6, it is possible to access node B. When a resistance is added at node B, such as the input resistance to another level of circuitry, a RC high-pass filter is created. For stimuli with frequencies below the cutoff frequency the film outputs a voltage proportional to the derivative of the input stimuli effectively differentiating the input signal. The 3dB frequency for the characteristic curve is governed by the equation $F_{3dB} = \frac{1}{(2*\pi*RC)}$, where R and C are values of the resistor and capacitor, respectively. Typical capacitance values for piezoelectric films are in the 10s to 100s of nano-farads (nF). Even for a very large resistance, the cutoff frequency is above 16Hz [37]. For lesser values of resistance, the cutoff frequency is in the hundreds and thousands of hertz. As discussed earlier in Section 3.2.2 almost all human motions are very low frequency. As a results the film can be used to sense the rate of change in angle of various joints such as the knee, elbow, and shoulder.

Because we are able to assume operation in frequency ranges much less than or much greater than the cutoff frequency, the film can be described by a simple mathematical model and the complex frequency based model can be avoided. A frequency-based model would require transformation of input data to the frequency domain via a Fast Fourier Transform

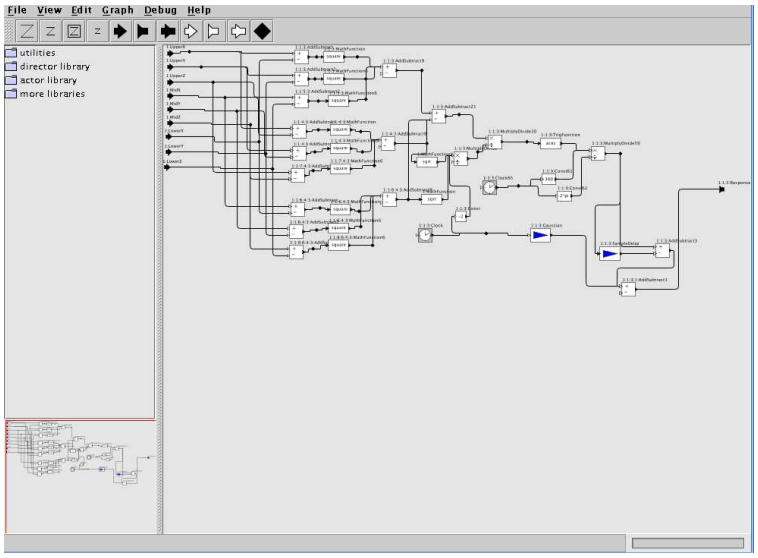

Figure 4.7: Ptolemy II model for a single piezoelectric film in the shape-sensing capacity

(FFT), the application of the characteristic filter equation, and the conversion of the signal back into the time domain using an inverse FFT. These operations are computationally expensive and can be avoided as a result of the operating assumptions. The output voltage, V_{out} of the sensor is dependent upon the piezoelectric coefficient corresponding to the type of stimulus, the amount of stress applied, and the thickness of the film. The equation for the film output voltage is $V_{out} = g_{3n}X_nt$ where g_{3n} is the piezoelectric coefficient, X_n is the applied stress, and t is the thickness of the film. This equation for the output voltage, however, is not useful for modeling the piezoelectric as an angular velocity sensor because calculation of the applied stress X_n is not feasible given just XYZ position data. Another method for modeling the sensor must be used.

With an understanding of the underlying sensor operation, the simulation model can be constructed. Due to the lack of force data, the simulation model is only capable of modeling the sensor as an angular velocity sensor, particularly targeted towards joints. The model of the film requires three XYZ triples (x_1,y_1,z_1,),(x_2,y_2,z_2,),(x_3,y_3,z_3,) that form a triangle ABC similar to that shown in Figure 4.4. A three-value sliding window technique similar to that found in the accelerometer model produces the next value for θ. The difference between each

successive value of θ is calculated generating the derivative θ'. This produces the angular velocity which is precisely what the sensor should detect. The difficulty lies in mapping the angular velocity values to their associated voltage output as the force characteristics are unknown. In addition to being difficult to map, it is just as difficult to generalize since the interface circuitry can have an effect on the scaling of the voltage. This problem was overcome by developing a scaling factor using voltages captured from an actual piezoelectric sensor output to determine what voltage values corresponding to various angular velocities. The scaling factor used for the models was approximately $\frac{2^\circ}{0.6V}$.

To ensure an accurate model was created, the pendulum platform used to verify the operation of the accelerometer was used. The piezoelectric film sensor was used to measure the angular velocity of θ as depicted in Figure 4.4. As derived earlier, the analytical equation for θ as a function of time is $\theta(t) = \theta_{MAX} * sin(\sqrt[2]{g/L} * t)$. The equation of interest is $\theta(t)' = \theta_{MAX} * g/L * cos(\sqrt[2]{g/L} * t)$. Output voltages from the film were recorded using a data acquisition card and compared to the analytical solution. The results, shown in Figure 4.8, confirmed that the model captured the general operation of a piezoelectric film sensor. While there was some deviation between the ideal and captured waveforms for the pendulum angle, it was clear that the sensor waveform was proportional to the angular rate of change and would likely be sufficient. Results discussed in Section 4.6.2 further solidify the validity of the model.

Another aspect of sensors that must be modeled is noise. Even in the presence of good design practices, noise is an inevitable part of real world applications. Noise can come from many sources such as non-decoupled analog/digital circuitry, electrical connections, and inherent sensor noise. In an effort to produce realistic sensor models and maintain the capability to analyze the effects of noise at the application level, Gaussian noise was included in both the accelerometer and piezoelectric sensor models.

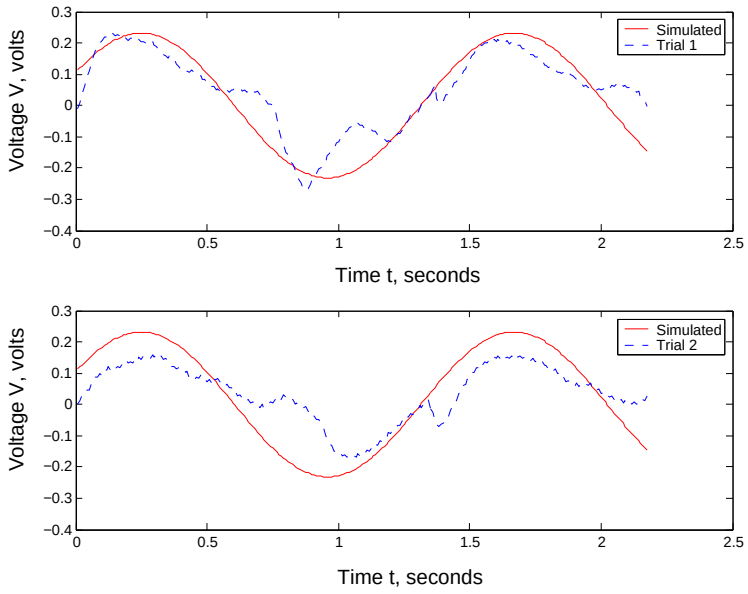

Figure 4.8: Verification of mathematical piezoelectric model using a pendulum

4.6 Modeling Applications

Having developed correct sensor models with a realistic source of driver data, applications can be explored and modeled.

4.6.1 Context Awareness

Development of the context awareness applications portion of the simulation environment consisted primarily of constructing methods for parameterizing the neural network, pre-processing algorithms, and post-processing algorithms. To avoid the overhead of implementing the different types of neural networks that could be used, the MATLAB Neural Network Toolbox (NNT) functions were utilized. Generalized MATLAB scripts were written that allowed the type of neural network, number of layers, layer functions, output type, and classifications to be easily varied.

To enable exploration of other design variables, feed-forward backpropagation was selected

as the primary type of neural network used in the simulations. Backpropagation networks typically, if trained correctly, excel at classifying inputs that they have not seen [43]. This property of backpropagation networks was considered important for dealing with variations in sensor input across populations. To get an idea for the size and complexity of the neural network required to identify various motions, a first-pass sensor set was selected to provide a test scenario. The test set of sensors consisted of accelerometers on the left and right hip coupled with piezoelectric films on the knees. For the first iteration, a test set of motions consisting of walking and running were selected as the recognition targets. Initial settings for the neural network were derived from examples in [32].

The first iteration network consisted of one input layer, four hidden layers, and an output layer. The size of the input layer is not necessarily equal to the number of sensor inputs. The pre-processing algorithm may produce multiple representations of each sensor. The pre-processing algorithm used must capture or extract underlying physical information that will give the neural network enough information to differentiate motions. Given the set of initial recognition target motions, walking and running, which are quite similar in form, the primary physical difference is the amount of energy in motion. Thus, the pre-processing method must capture this difference in energy. The initial pre-processing algorithm chosen was the average of the absolute value over a sliding window. The window size used must capture enough information about the motion. A sliding window that is too small will provide too much granularity, a sliding window too large will spread across multiple instances of a motion. The window must be able to capture the slowest motion. The slowest motion in the initial motion set is walking. A single step takes approximately 0.5 seconds. Given the 120Hz sampling rate of the human motion source data, a sliding window of size 60 was used. The layer functions were chosen to be the Tan Sigmoid transfer function *tansig* governed by the equation $tansig(n) = (2/(1 + \exp -2 * n)) - 1$. Tan Sigmoid transfer functions were selected because they are differentiable which is required for backpropgation networks. Other differentiable transfer functions exist such as the Log Sigmoid, however Tan Sigmoid is most commonly used [31]. Note that the function is bounded by +1 and -1. The input values to

the neural network must be normalized to fit within this range after being preprocessed. The neural network was trained using the resilient backpropagation algorithm *trainrp* included in the MATLAB NNT. This algorithm was chosen for its speed and ability to handle problems associated with the *tansig* function and the steepest decent training method [43]. Specifically, the resilience of the algorithm is its ability to ignore changes to the neuron biases that are too small. This type of behavior is an artifact of the training functions.

The training process consisted of the following steps:

- **Retrieve sensor data for all data sets**
- **Pre-process using sliding window**
- **Normalize between +1, -1**
- **Create target vectors**
- **Train**

The first attempt at training the neural network encountered a minor problem associated with the method of presentation of the training vectors to the neural network. Sensor data from each training set was appended and processed in order. For example, given data sets $walk_1$, $walk_2$, run_1, run_2, the neural network would be presented with all walking data before ever encountering running data. This caused the neural network to become over trained to a particular input. To resolve this, contiguous samples of equal sizes were extracted from each data set, pre-processed, and randomly presented to the neural network. Using this method produced far better training results. A similar issue was encountered when there were many more input data files of a certain motion type. As a result, the number of files for each type of training motion were kept as even as possible given data set availability.

A neural network with sufficient recognition capabilities was developed using an iterative train-evaluate process. This allowed the neural network variables to be fixed such that the

exploration of other design variables could occur. The finalized neural network contained one input layer of eight neurons, five hidden layers of ninety-six,forty-eight, twenty-four, twelve, and six neurons, and one output layer of three neurons. Classification vectors were provided as integers, but were converted to binary representations to accommodate the limits of the *tansig* layer function. Basic summation across the sliding window was added as a pre-processing function to resolve between similar motions such as sitting and standing that differ only in direction.

4.6.2 Gait Analysis

As discussed in Section 3.2, gait analysis requires the measurement of several dependent variables. The majority of the variables reside in the velocity and displacement domains. The accelerometers provide the first and second derivatives of these two domains, respectively. To calculate velocity and displacement, acceleration must be integrated. Typically, integration of accelerometer data is cautioned against due to the accumulating error effect caused by sensor noise [44] and the unknown initial velocity/position constant. For any relatively lengthy integration interval ,this rule is generally true. However, for shorter time intervals it is possible to successfully integrate accelerometer data. The boundaries for lengthy and short integration intervals depends heavily on the amount of sensor noise and for this reason is not firm. This concept can be extended to other sensors such as the piezoelectric films.

Because gait analysis requires accurate calculation of necessary variables from raw sensor data, previously discussed issues such as sensor orientation change must be fully considered. The application, unlike the sensor models, does not have access to all of the raw position data. Instead, the application is privy only to the transformation of the position performed by the sensor models. Because the sensors models have access to all of the position data it was possible to correct the ideal sensor output for situations such as orientation change as discussed in Section 4.4. The application, however, must perform the reverse operation of mapping the corrected sensor output to the ideal sensor output without the luxury of

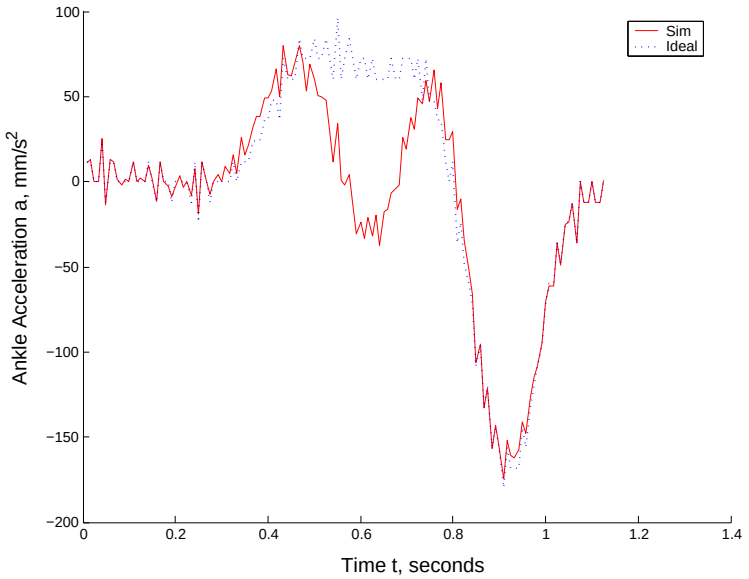

Figure 4.9: Ideal and orientation-corrected ankle acceleration curves

additional information.

Given that the modeled e-textile was a pair of pants, the particular scenario that required this type of correction was the accelerometer placed on the ankle. During normal (non-shuffled) steps, the ankle accelerometer changes orientation on the back swing phase of the step such that the horizontal axis of the accelerometer is influenced by vertical motion and vice versa. This effect produced significant deviation when compared to the ideal as shown in Figure 4.9. Fortunately, the interval of deviation is small and continuous. Calculation of the velocity and step length using the simulated accelerometer produced significant error as shown in Figure 4.6.2. To calculate accurate gait metrics, it is necessary to compensate for the deviant acceleration.

The basic biomechanics of a step dictate that the initial velocity and termination velocity of a step must be approximately zero. The velocity curve calculated using the simulated accelerometer shown in 4.11 has a termination velocity that is non-zero. This discrepancy is exploited to produce a three-point piecewise, linear fit across the affected interval of the ankle acceleration that substantially corrects the curve. A two-point linear fit was considered,

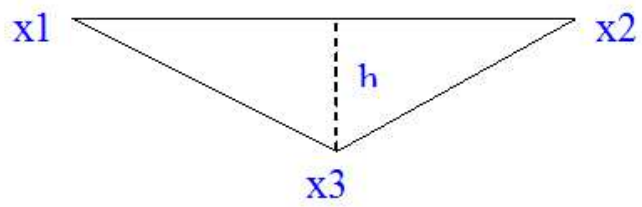

Figure 4.10: Triangle measurement used in the fitting algorithm

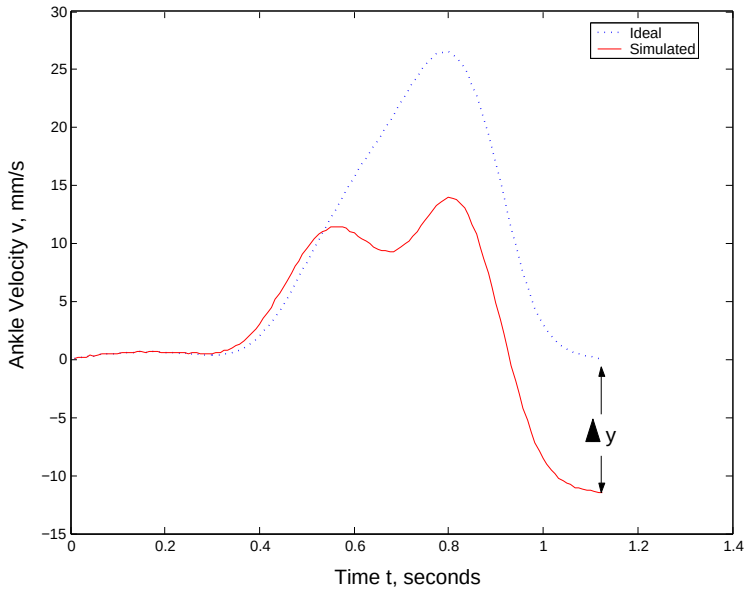

Figure 4.11: Velocity curves generated via integration of ideal and orientation-corrected accelerations in Figure 4.9

however the three point piecewise linear fit generally produced less error. The beginning and end of the affected interval is identified (usually as peaks) and a line is fit between the two points, $x1$ and $x2$. The portion of the curve before $x1$, the newly fitted line, and the portion of the curve after $x2$ are retained to form a composite acceleration curve. This curve is then integrated to obtain velocity. The difference in the final velocity with respect to the ideal case of zero, Δy, is shown in Figure 4.11.

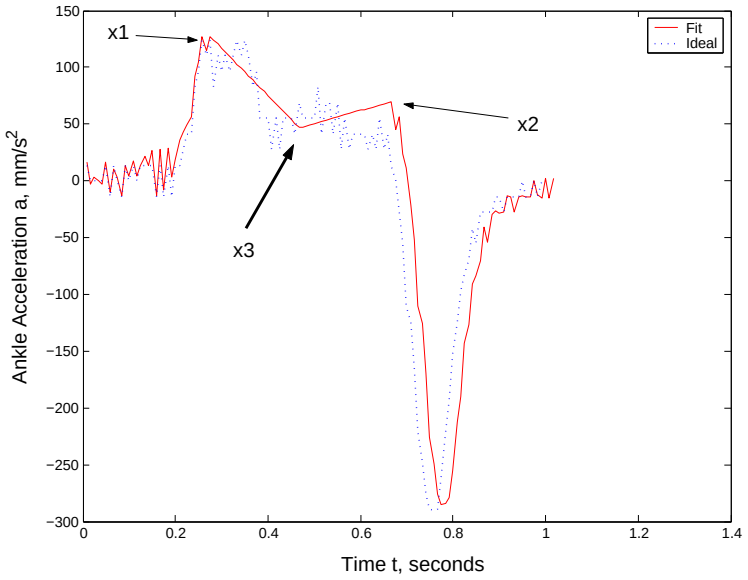

Figure 4.12: Fitted and ideal ankle acceleration curves

The midpoint, $x3$, of $x1$ and $x2$ is calculated. A triangle is created from the points $x1$, $x2$, and $x3$ with a variable height, h defined as the difference from the line previously formed by $x1$ and $x2$ depicted in Figure 4.10. The area of this triangle is set equal to Δy and h is calculated. Two new lines are created using the pairs $(x1, y1)$, $(x3, y3)$ and $(x2, y2)$, $(x3, y3)$ and a second composite acceleration curve is created using pre-interval and post-interval segments and the newly created lines shown in Figure 4.12. This new curve, when integrated to find velocity and step difference, is far more accurate and shown in Figure 4.13.

The step lengths for four subjects (two steps per subject) were calculated via simulation using the ideal motion capture position data, simulated accelerometer, and the three-point

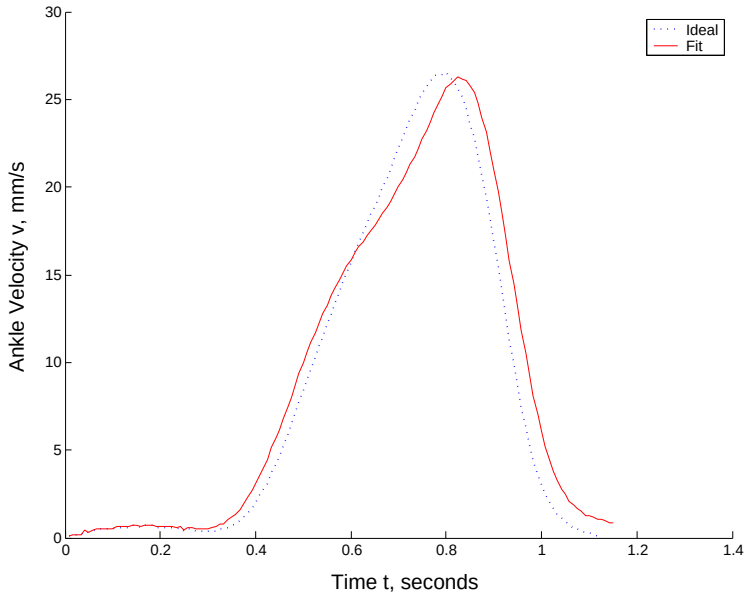

Figure 4.13: Velocity curves generated via integration of ideal and fitted accelerations in Figure 4.12

piecewise linear fit method described above. Because calculation of velocity is required to calculate displacement, step length was selected a a primary metric for success. The ability to accurately calculate step length implies that velocity must also be accurate which enables a variety of other measurements. The resulting calculations using the fitted curve had an average error of 7% from the ideal value calculated from position data as shown in Table 4.6.2. Uncorrected acceleration data averaged 71% error. The consistency of the final error with the fit had a standard deviation of 1.1%. This indicates that the error is fairly consistent across different measurements. Looking at Figure 4.13 it is clear that while the fitting method greatly improves the calculation the fitted velocity curve slightly deviates from the ideal. This slight deviation is a likely source for the error. Because the models attempt to simulate the actual physical sensors they too are limited by the physical characteristics of the selected devices. If greater accuracy was required, the selected sensors could be replaced with superior devices (assuming existence), the fitting method could be refined, or additional sensors could be added to assist in resolving the orientation of the foot during the step cycle.

(subject)	Actual (mm)	Sim (mm)	Fit (mm)	Sim Err %	Fit Err %
Step 1 (1)	1097.4	341.2	1175.2	-68.9	7.1
Step 2 (1)	1084.4	413.6	1159.7	-61.9	6.9
Step 1 (2)	1180.6	271.3	1251.2	-77	6
Step 2 (2)	1172.4	318.7	1267.8	-72.8	8.1
Step 1 (3)	1220.8	312.5	1323.0	-74.4	8.4
Step 2 (3)	1234.1	303.6	1343.2	-75.4	8.8
Step 1 (4)	1410.3	299.6	1524.9	-78.8	8.1
Step 2 (4)	1411.3	512.2	1489.4	-63.7	5.5

Table 4.1: Step length and error calculations using simulated sensors with and without fitting method

The validation of the sensor models using the pendulum apparatus provided a consistent platform for verification of the sensor models. With verified sensor models, the development of methods for virtual sensor translation and orientation correction were confidently created. The ability to place sensors throughout the surface of the body, limited only by the inclusion of points in the human motion data, produced a very flexible environment for simulation and application development. Additionally, orientation correction not only allowed correct calculation of step length but was achieved without the addition of sensors. The results for both the accelerometer, piezoelectric films, and associated calculations indicate that the models are accurate enough to provide reasonable measurements for the desired applications.

Chapter 5

Validation & Results

For simulations to be useful they must be grounded in reality. This chapter verifies and validates the realism of the simulation and discusses results stemming from its application. The first portion of the chapter compares data from simulation and data taken from the prototype e-textile. The second portion focuses on the use of simulation to explore several design variables. The remainder of the chapter discusses the simulation and prototype results of the context awareness and gait analysis applications.

5.1 Verification

The prototype e-textile pants discussed in Section 3.3 were utilized as the primary method for validating the simulation. Data was collected from the prototype e-textile during a videotaped motion capture session, allowing for the comparison between the data collected from the prototype e-textile pants and the output of simulation when driven by the motion capture data. Specifically, prototype data was collected from accelerometers on the ankle and piezoelectric films located at the knee joints. The points of interest on the body captured using the motion capture system were the heels, ankles, knees, and hips.

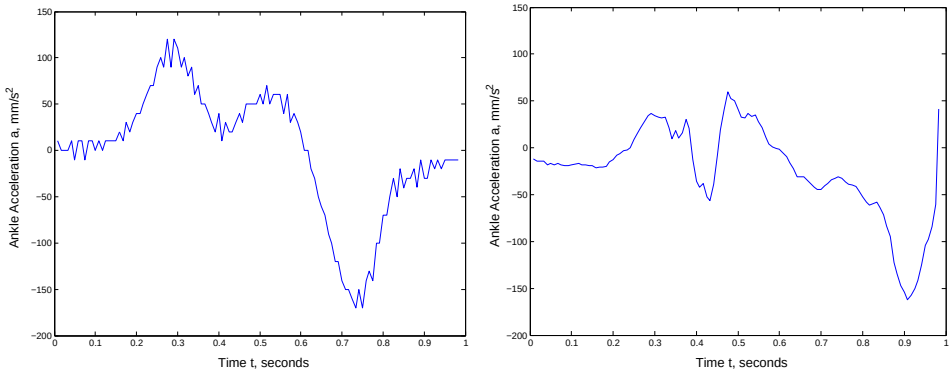

Figure 5.1: The figure on the left (a) depicts simulated accelerometer output when placed on the ankle. The figure on the right (b) depicts ankle accelerometer data collected from the prototype e-textile

The ankle was selected as the site for the validation test due to its high degree of freedom. Obtaining correct results on a portion of the lower body with fewer degrees of freedom such as the knee would have been significantly easier and would not have incorporated the orientation change mechanism. Real and simulated accelerometer curves are shown in Figure 5.1 (a) and (b). The curves shown in Figure 5.1 are not from the same step and are intended to emphasize similar curve shape. While the data taken from the motion capture session was reasonable enough to perform calculations, it was not clean enough for a precise graphical comparison of accelerometer output shown in Figure 5.1. Note that the shape and features of the curves are quite similar.

The matching accelerometer curves verified that the model sufficiently captured reality. The simulated and real accelerometer curves were not directly compared (i.e. calculating error between the two curves) due to uncertainties in synchronization of the two data sources and because required accuracy is application dependent. It was clear from graphical comparison that the model was sufficiently accurate for the gait analysis and context awareness applications.

Real and simulated piezoelectric curves are shown in Figure 5.2 (a) and (b). These graphs differ only in the occasional negative spike. This spike was an artifact of the vibration result-

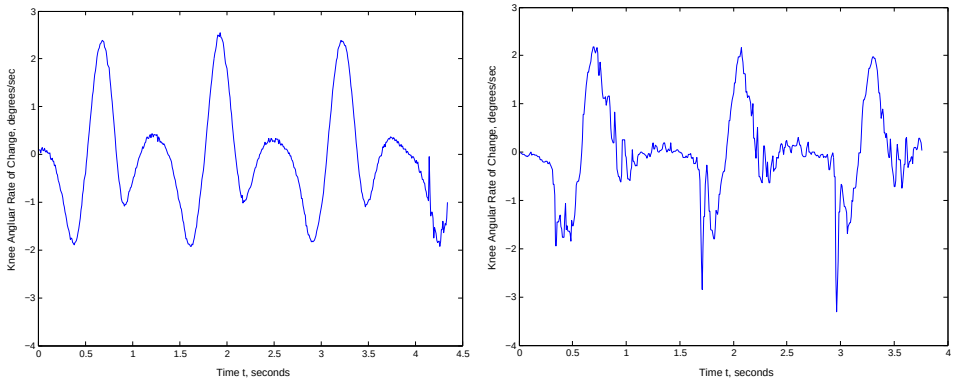

Figure 5.2: The figure on the left (a) depicts simulated output from a piezoelectric film placed on the knee. The figure on the right (b) depicts real data collected from a knee-positioned piezoelectric film on the prototype e-textile

ing from the heel strike and was not a major deviation. The simulated and real piezoelectric film curves indicate a correct model that is reasonable for the gait analysis application. Again, direct comparison was not performed due to synchronization uncertainty and application dependent accuracy requirements. Graphical comparison indicated that the models were sufficient for the gait analysis and context awareness applications.

5.2 Design Exploration Using Simulation

As mentioned in Chapter 4, simulation provides the ability to explore the design space prior to the construction of prototypes. The first design issue investigated with simulation was the variation of dynamic sensor range across different points of the body. Since the prototype dealt primarily with the lower body, only the waist and lower limbs were considered. Accelerometers were simulated on the hip, knee and heel points. The horizontal accelerations for each point are shown in Figure 5.3. The range of acceleration at the ankle is nearly an order of magnitude greater than that of the hip. This is an important consideration when designing interface circuitry. The circuitry can be specialized for each case to obtain maximum resolution, or can be generalized such that one design can be used across all of the

sensors.

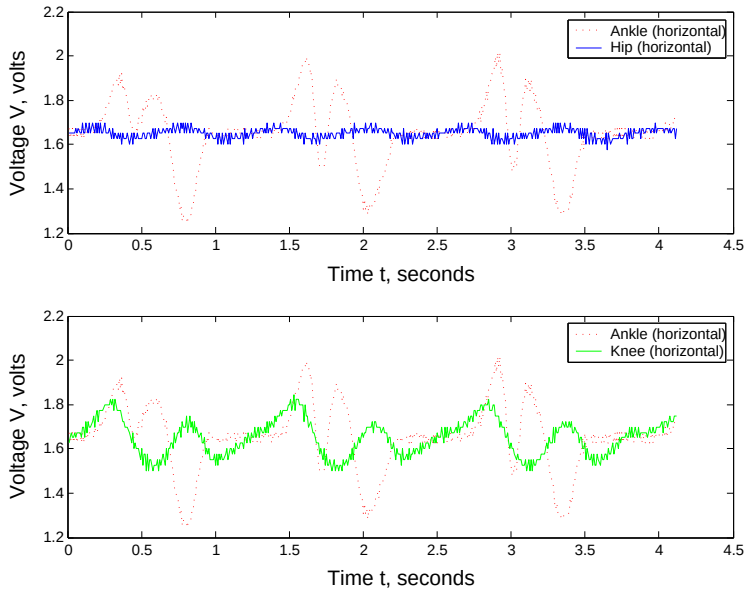

Figure 5.3: Comparison of dynamic sensors ranges associated with different portions of the body

The second design variable explored with simulation was the effect of sensor placement variation. Deviation of sensor placement from the ideal or desired placement can impact applications and dictate the number of required garment sizes. Examples of this phenomenon include an accelerometer several inches out of ideal position due to a short pant leg or a piezoelectric sensor not centered on the knee. Figure 5.4 shows the responses of an accelerometer at varying points on the lower leg between the ankle and knee. As the accelerometer is displaced further from the ankle joint the response curves approaches that of the knee joint. At the center-point between the ankle and knee the curve is the average of the ideal ankle and knee responses. Significant deviation from the ideal ankle response occurs when the deviation exceeds 20%-15% of the total distance. Similar behavior was observed when the effects of sensor deviation on context awareness application was explored in Section 5.3. The number of garments required can be gleaned from this information and specific application requirements.

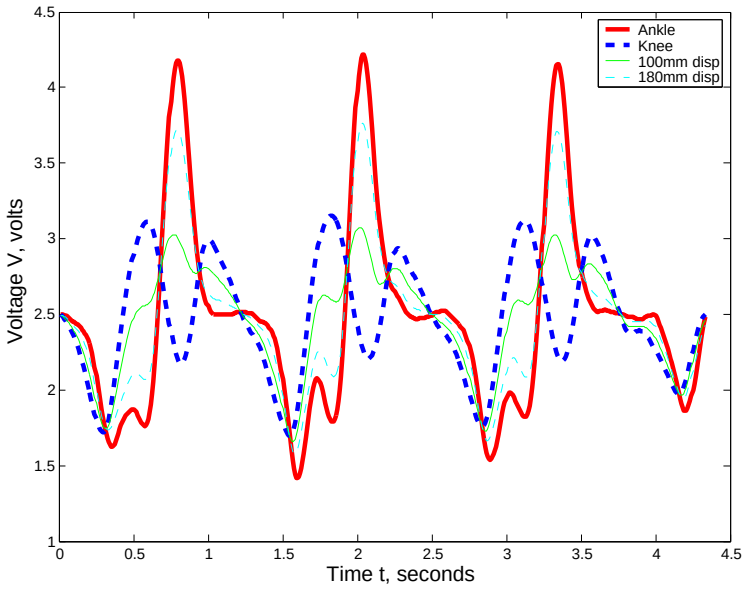

Figure 5.4: Effects of sensor translation on sensor output response between the ankle and knee

Another important aspect of designing wearable electronic textiles is variation of sensor output across body sizes. For example, the range of acceleration at the knee for a short female may differ greatly from an extremely tall male. Simulation was used to determine if this type of variation was a significant concern. Figure 5.5 depicts the maximum and average accelerations for twenty subjects with increasing leg sizes. This experiment indicates that body size and acceleration range is not highly correlated. In fact, there happens to be a slightly *negative* trend. Consequently, variation of sensor output across body size was not a significant design consideration.

5.3 Context Awareness

In addition to general design variables associated with wearable electronic textiles, specific applications may be explored and/or designed using simulation as discussed in Section 4.6.1. Of primary importance when designing the context awareness application was generalization

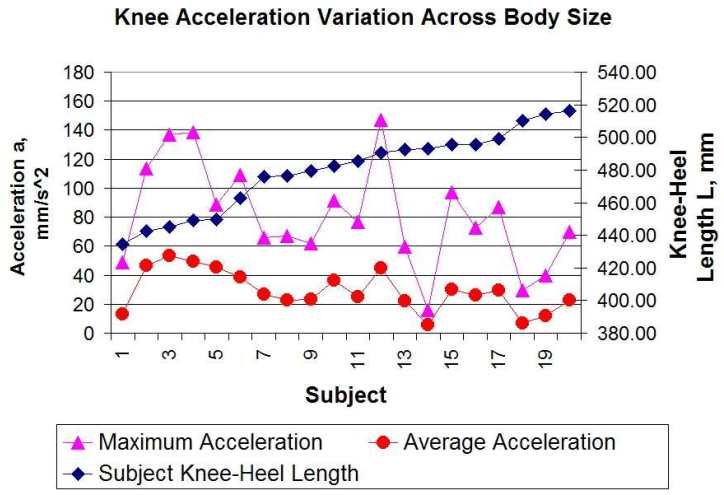

Figure 5.5: Effects of body size on sensor output

across an entire population. Many previous context awareness applications such as [16] [18] were trained on a small number of people. Simulation offers the ability to train on a large number and wide variety of people. To minimize design effort the affects of the training population on generalization needed to be understood. An experiment was performed which tested five possible training population scenarios. Because activities such as walking and running were of interest, the heel acceleration was used as the variable for segmenting the population. The five training scenarios were as follows: one subject with average acceleration, once subject with the lowest acceleration, one subject with the highest acceleration, two subjects with average acceleration, two subjects each with outlying (high and low) acceleration. The results of the simulation are shown in Figure 5.6. The training set that displayed the greatest level of generalization was two subjects with average acceleration. Training on two outliers also performed reasonably well.

Additional variables that have an effect on the accuracy of the context awareness application were explored such as pre-processing window size variation and sensor placement variation. Variation in the pre-processing window may be caused by variations in sampling rate. Figure 5.7 shows the accuracy of the context awareness application as the pre-processing window size was varied from one to three-hundred. The neural network used for the eval-

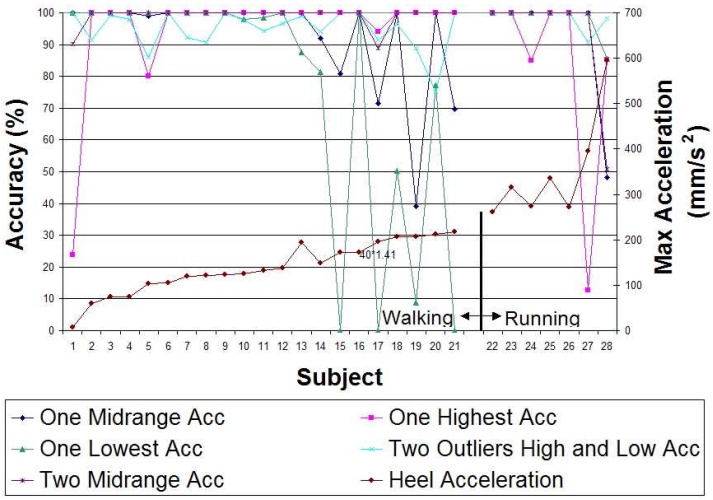

Figure 5.6: Effects of training population on the accuracy of the context awareness application

uation was trained using pre-processing windows of size sixty-four. Note that as expected, maximum accuracy is obtained with the window size used to train the neural network. Sensor placement variation, similar to that discussed in Section 5.2, also affected the accuracy of the neural network as shown in Figure 5.8. Given the knee-ankle distance of 500mm, note that the neural network accuracy begins to degrade at around 125-150mm of displacement or approximately 30% error. This type of information can be quite useful when determining the number of required garments and/or evaluating application variations.

While exploration of individual design variables provides insight into the behavior of the context awareness application, the combined effects of multiple variables must also be explored. To illustrate this concept the simulation environment was used to find a near-optimal sensor configuration given a set of constraints and was used to explore the robustness of various configurations to sensor placement deviation. The experiment was constrained to four sensors (two piezoelectric films and two accelerometers) and three primary placements points (hips, knees, ankles). These constraints mimicked the available prototype hardware and encompassed important points on the body. Given two sensor types and three placement points, six configurations are possible. Analysis of sensor data showed that placing the

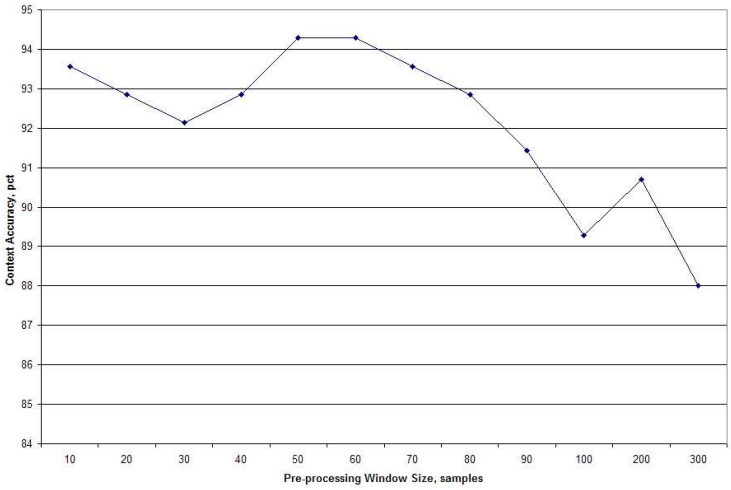

Figure 5.7: Effects of pre-processing window size on context awareness application accuracy

accelerometers on the hips is not useful, since the accelerations at the hip are too small to fully resolve using current accelerometer technology. This narrows the exploration to four configurations. Each configuration was evaluated by training the neural network using the configuration and testing the performance of the neural network with 0mm (0 inch), 75mm (3 inches), and 150mm (6 inches) displacements of sensors from their desired positions. Since piezoelectric films are resilient to displacements, the displacement operation was performed solely on the accelerometers. The zero displacement case shows best case performance while the other two cases provide insight to the robustness of the context awareness application to sensor deviation. Table 5.1 shows the results of this experiment. The worst configuration was piezoelectric films on the ankle joints and accelerometers on the knees. This configuration achieved a maximum accuracy of 80% and deviated as much as 6.25% when the accelerometers were displaced 150mm. The best configuration was piezoelectric films on the knees and accelerometers on the ankles. This configuration achieved a maximum accuracy of 97.5% and deviated 8.25% when the ankle accelerometers deviated 75mm. These results show that the knee ankle arrangement is robust to sensor deviation.

To further explore the design space. The same experiment was performed however the neural network was emphre-trained for each configuration and deviation trial. This experi-

Placement		Accuracy (pct)		
Piezoelectric	**Accelerometer**	**0**	**75mm**	**150mm**
knees	ankles	97.5	88.7	92.5
hips	ankles	82.5	80.0	81.2
hips	knees	80.0	77.5	78.7
ankles	knees	80.0	86.2	73.7

Table 5.1: Context recognition accuracy for four scenarios where neural network is testing using displaced sensors

Placement		Accuracy (pct)		
Piezoelectric	**Accelerometer**	**0**	**75mm**	**150mm**
knees	ankles	97.5	91.2	98.7
hips	ankles	82.5	87.5	78.7
hips	knees	80.0	75.0	80.0
ankles	knees	80.0	83.7	82.5

Table 5.2: Context recognition accuracy for four scenarios where neural network is re-trained using displaced sensors

ment evaluated the quality of sensor placements beyond the primary placement points. Table 5.2 shows the results of this experiment. Improvements in recognition accuracy were made in almost every scenario. Again, the piezoelectric films on the knees and accelerometers on the ankles configuration performed the best. This configuration was selected as the near-optimal configuration. In simulation this configuration achieved a maximum accuracy of 97.5%. Using the same neural network (trained on simulation) with the prototype e-textile, recognition accuracy between 75%-85% were observed. It should be noted that these stated accuracy values were gleaned from raw neural network output. More robust context awareness applications might include Markov chains or a state machine to manage the raw neural network output. Refinement of the application was beyond the scope of this work.

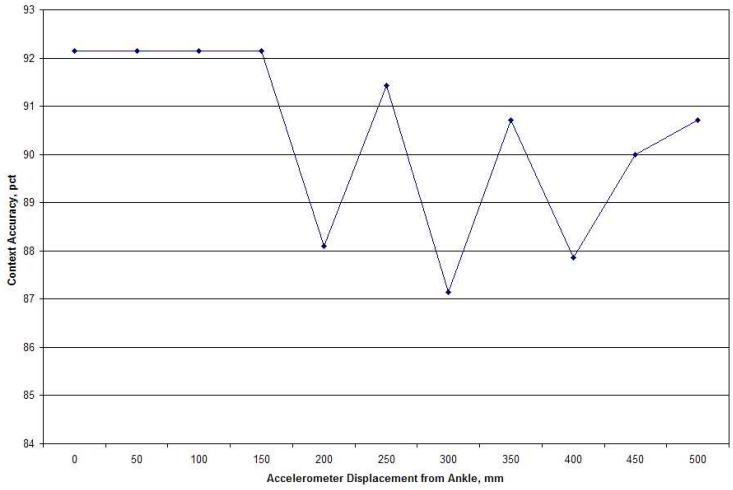

Figure 5.8: Effects of sensor placement variation on context awareness application accuracy

5.4 Gait Analysis

Having previously verified correct operation of the accelerometer and piezoelectric sensors, calculating most required gait analysis parameters is fairly simple. Accelerometer data can be integrated over relatively short periods of time to obtain velocities and displacements. This lends nicely to the calculation of step length, heel strike velocity, slip distance, and sliding heel velocity. Table 5.4 shows step lengths calculated using accelerometer data from the prototype e-textile and compared to the actual value calculated using video data. The error encountered was similar to the values calculated via simulation in Table 4.6.2.

Heel strike velocity was calculated by integrating acceleration during the heel strike period, defined as the period of time between $\frac{1}{60th}$ of a second before and after heel contact. Because of the dual axis nature of the accelerometer the horizontal and vertical heel strike velocities can be calculated independently and/or combined to provide a velocity vector. Figure 5.9 depicts the heel strike velocity during a typical step calculated using data from the prototype e-textile. If desired, the heel strike interval could be detected using piezoelectric films on the heel. In addition to heel strike interval information piezoelectric films can provide information similar to force plate data when placed on the heel or other parts of the foot. Figure 5.10

(subject)	Actual (m)	Fit (m)	Err %
Step 1 (1)	1.31	1.41	7.57
Step 2 (1)	1.41	1.31	-6.89
Step 1 (1)	1.33	1.32	-1.28
Step 2 (1)	1.39	1.38	-0.72

Table 5.3: Step length calculation using data from the prototype e-textile and verifying using motion capture data

shows the typical output of a piezoelectric film placed on the bottom of the heel during the heel strike phase of the step superimposed with the force plate data for the same step. Note that the piezoelectric film can be used to accurately calculate the step forces. Piezoelectric films may be used to replace force plates, focus data collection on a certain area of interest, or provide further information when accelerometers are not sufficient. The slight phase shift in the piezoelectric film and force plate curves is an artifact of the placement of the film. The film was placed on the back edge of the shoe which experiences the transfer of force earlier in the step motion.

The results presented demonstrate the use of simulation for exploration of the design space and application development. Results from the prototype e-textile verify the correct operation of the simulation and validates its use in application design and design space exploration.

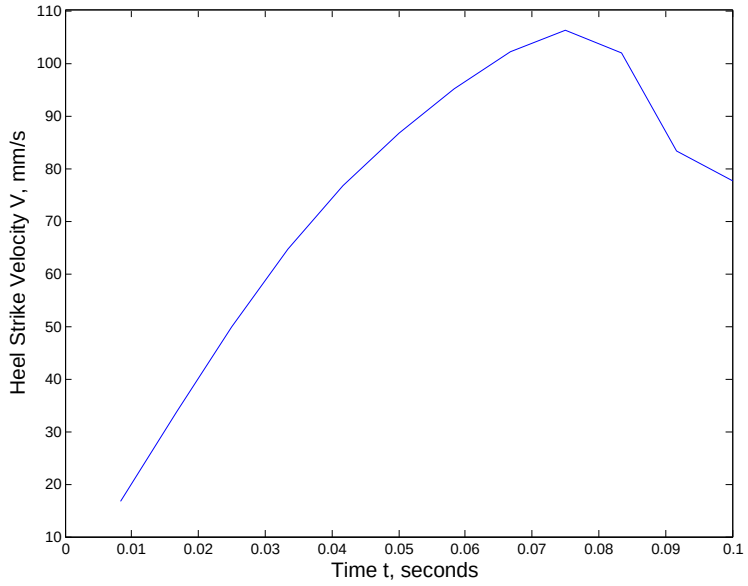

Figure 5.9: Heel strike velocity curve via integration of accelerometer data

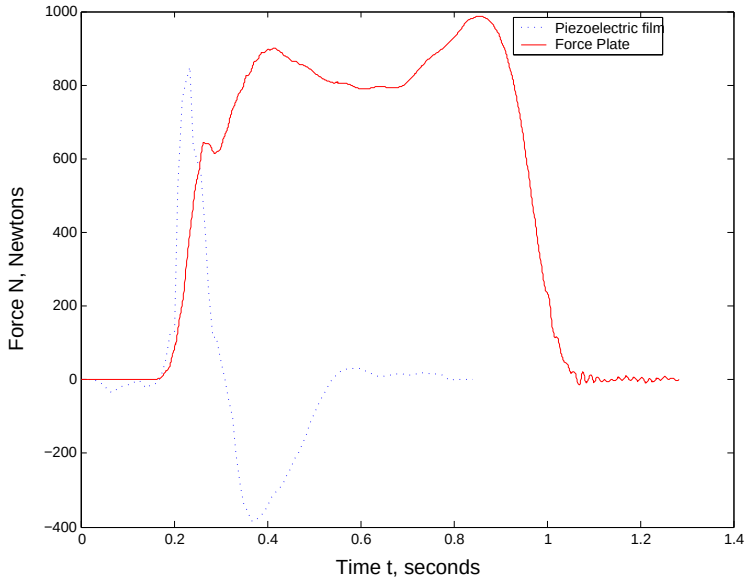

Figure 5.10: Step force sensing using piezoelectric films on the heels

Chapter 6

Conclusions

The relationship between textiles and the human body provides a natural foundation for wearable e-textiles. As presented, simulation allowed not only for exploration of the enormous design space associated with human factors but also produced a robust application design with a single prototype iteration. Additional benefits of simulation shown to be useful are exact repeatability of experiments, removal of human test subjects, and greater testing/training population size. Exploration of the design space included investigation of population variation effects on sensor output, sensor placement variation, and other parameters that affect wearable design. Exact repeatability of experiments assisted in debugging and enhanced algorithm development. Removal of human subjects alleviated the hassle associated with human testing. Increased testing/training population allowed for generalization and assured that the application would operate correctly across many people. The simulation environment presented is also extendable allowing the addition of more sensors, improved models of existing sensors, and/or models for newer, more precise sensors. Independence from the source data encourages expansion using additional motion capture data or animation data to drive the sensor models. The results from the pendulum and prototype e-textile applications indicate that the simulation effectively mapped to reality and was successfully used to develop the context awareness and gait analysis applications.

Prototypes designed using simulation were capable of performing the desired applications and served as verification of the simulation. The two applications chosen as case studies, context awareness and gait analysis, emphasized the validity of e-textiles in wearable applications and demonstrated two areas in which e-textiles can have an immediate impact. Successful design of an application primarily in simulation is showcased via the context awareness application. The ability to exactly repeat scenarios eliminated variables from the development process, in this case, the design of the neural network. In addition to the neural network design, the effects of various sensor and computation variations on the application were effectively explored. Training of the neural network using a large population and exploring different subsets of the population improved overall accuracy.

Highlighting e-textiles as an accurate method of sensor deployment was the gait analysis application. The gait analysis application achieved 7% (approximately 1 cm) error in step length calculations. While 7% error is non-trivial, it is not directly attributable to the e-textile itself. Other factors such as sensor noise and fitting algorithm may be to blame. Pinpointing of the error and refinement of the application are possible points for future work. In addition to movement-related data collection, the the e-textile allowed the collection force data using piezolectric flims as force sensors. Successful sensing of these types of parameters strengthens the case for e-textiles in motion analysis/health applications. The ability to collect accurate gait/locomotion information in a natural and portable device may, in the future, enhance gait analysis, elderly monitoring, biomechanical study, sports medicine, and a host of other applications. Additionally, the low cost of e-textiles when compared to current systems used in gait-related applications may provide greater access to technology.

The most convincing indicator of the importance of simulation in the design of wearable e-textiles and the success of this thesis was the correct operation of the first prototype. Without simulation and the benefits it provides, a working first-iteration prototype would have been unlikely. The simulation environment, applications, and associated results serve to show that the motivation and stated contributions of this thesis have been satisfied.

6.1 Future Research

Future research in the area of wearable e-textiles falls into two distinct categories: mechanical and computational. Mechanical issues involved in e-textiles include miniaturization of electronic components, improving the integration of electronic components with the textiles, and refining the devices used to connect sensing nodes to the fabric. Textile related problems such as garment construction using electrically-capable fabrics, integration of wires, and fashion are other mechanical-related problems. Computational issues include development of a method for easily modifying the target application, architectures for processing data, and refined algorithms for deriving highly abstracted inferences from low-level sensor data. Other optional computation features such as distributed processing using embedded systems, reconfigurable computing in embedded devices maybe be required to fully enable e-textiles for non-specialized applications. For e-textiles to be widely accepted ease of use must also be achieved.

Bibliography

[1] S. Park, C. Gopalsamy, R. Rajamanickam, and S. Jayaraman, "The wearable motherboard: An information infrastructure or sensate liner for medical applications," *Studies in Health Technology and Informatics, IOS Press*, vol. 62, pp. 252–258, 1999.

[2] J. Farringdon, A. Moore, N. Tilbury, J. J. Church, and P. Biemond, "Wearable sensor badge and sensor jacket for context awareness," in *Proceedings of the Third International Symposium on Wearable Computing.* ISWC 1999, October 1999, pp. 107–113.

[3] J. Edmison, M. Jones, Z. Nakad, and T. Martin, "Using piezoelectric materials for wearable electronic textiles," in *Proceedings of the Sixth International Symposium on Wearable Computing.* ISWC 2002, 2002, pp. 41–48.

[4] Z. S. Nakad, "Architectures for e-textiles," Ph.D. dissertation, Bradley Department of Electrical and Computing Engineering, Virginia Tech, 2003.

[5] E. Post, M. Orth, P. Russo, and N. Gershenfeld, "E-broidery design and fabrication of textile-based computing," *IBM Systems Journal*, vol. 39, no. 3 and 4, pp. 840–860, 2000.

[6] R. Paradiso, G. Loriga, N. Taccini, M. Pacelli, and R. Orselli, "Wearable system for vital signs monitoring," in *International Workshop on New Generation of Wearable Systems for eHealth*, December 2003, pp. 161–168.

[7] F.-C. Chan, F. Dabiri, R. Jafari, E. Kursun, V. Raghunathan, T. Schoellhammer, D. Sievers, D. Estrin, G. Reinman, M. Sarrafzadeh, M. Srivastava, B. Wu, and Y. Yang, "Reconfigurable fabric: An enabling technology for pervasive medical monitoring," in *Proceedings of Communication Networks and Distributed Systems: Modeling and Simulation*, January 2004.

[8] T. Sheikh, "Modeling of power consumption and fault tolerance for electronic textiles," Master's thesis, Bradley Department of Electrical and Computing Engineering, Virginia Tech, 2003.

[9] R. Parker, R. Riley, M. Jones, D. Leo, L. Beex, and T. Milson, "Stretch - an e-textile for large-scale sensor systems," in *International Interactive Textiles for the Warrior Conference*, 2002, p. 59.

[10] R. Shenoy, "Design of e-textiles for acoustic applications," Master's thesis, Bradley Department of Electrical and Computing Engineering, Virginia Tech, 2003.

[11] Burton, "Snowboard Jacket with SOFTSwitch Keyboard," 2004, http://www.burton.com/Burton/gear/products.asp?productID=728.

[12] SOFTSwitch, "SOFTSwitch Electronic Fabrics," 2004, http://www.softswitch.co.uk/.

[13] S. Jung, C. Lauterbach, and W. Weber, "Integrated microelectronics for smart textiles," in *Workshop on Modeling, Analysis, and Middleware Support for Electronic Textiles*. MAMSET 2002, October 2002.

[14] P. Grossman, "The lifeshirt: A multifunctional ambulatory system that monitors health, disease, and medical intervention in the real world," in *International Workshop on New Generation of Wearable Systems for eHealth*, December 2003, pp. 73–80.

[15] Eleksen, Ltd., "http://www.eleksen.com," 2004.

[16] K. V. Laerhoven and O. Cakmakci, "What shall we teach our pants?" in *Proceedings of the Fourth International Symposium on Wearable Computing.* ISWC 2000, October 2000, pp. 77–83.

[17] A. Golding and N. Lesh, "Indoor Navigation Using a Diverse Set of Cheap Wearable Sensors," in *ISWC*, 1999, pp. 29–36.

[18] C. Randell and H. Muller, "Context awareness by analysing accelerometer data," in *Proceedings of the Fourth International Symposium on Wearable Computing.* ISWC 2000, October 2000, pp. 175–176.

[19] H. G. K. Van Laerhoven, A. Schmidt, "Multi-sensor Context Aware Clothing," in *ISWC*, 2002, pp. 49–57.

[20] B. Clarkson, K. Mase, and A.Pentland, "Recognizing user context via wearable sensors," in *Proceedings of the Fourth International Symposium on Wearable Computing.* ISWC 2000, October 2000, pp. 69–75.

[21] Merriam-Webster, "Merriam-Webster Online Dictionary," 2004, http://www.m-w.com/.

[22] Motion Analysis Corporation, "Motion Analysis," 2004, http://www.motionanalysis.com/index.html.

[23] Insight Product Development, "Insignt Product Development: Interface Design," 2004, http://www.insightpd.com/.

[24] Kinematics Laboratory of Ottawa, "Biomech Motion Analysis Software," 2004, http://www.health.uottawa.ca/biomech/csb/software/biomech.htm.

[25] T. Lockhart. (2004) Human Factors Engineering and Ergonomics Center. [Online]. Available: http://hfec.vt.edu/labs/loco/loco.htm

[26] CSMI Inc., "HUMAC/CYBEX Norm Systems," 2004, http://www.csmisolutions.com/humac/humacnorm.shtml.

[27] T. Davis and T. E. Lockhart, "Relationship Between Age and Anxiety on the Biomechanics of Slips and Falls," in *The Proceeding of the XVI Annual International Society of Occupational Ergonomics and Safety (ISOES)(Session 5-1)*, 2002, pp. 1–5.

[28] S. Kim and T. E. Lockhart, "Effects of age-related changes in hamstring activation rate and heel contact velocity on the biomechanics of slips and falls," in *The Proceeding of the XVI Annual International Society of Occupational Ergonomics and Safety (ISOES)(Session 5-2)*, 2002, pp. 1–5.

[29] U. V. Cunha, "Differential Diagnosis of Gait Disorders in the Elderly," in *Geriatrics vol. 43*, pp. 33–38.

[30] UC Berkeley, EECS, "Ptolemy Project: Heterogeneous Modeling and Design," http://ptolemy.eecs.berkeley.edu/index.htm.

[31] Mathworks, "MATLAB Neural Network Toolbox," 2004, http://www.mathworks.com/products/neuralnet/.

[32] ——, "MATLAB Help," 2004, http://www.mathworks.com.

[33] D. Lehn, C. Neely, K. Schoonover, T. Martin, , and M. Jones, "e-TAGs: e-Textile Attached Gadgets," in *Proceedings of Communication Networks and Distributed Systems: Modeling and Simulation*, January 2004.

[34] Microchip Corporation, "PICmicro Mid-Range MCU Family Reference Manual," 2004, http://www.microchip.com/.

[35] Atmel Corporation, "AVR 8-Bit RISC Products," 2004, http://www.atmel.com/products/AVR/.

[36] Analog Devices Inc., "ADXL311 Dual-Axis Accelerometer," 2004, http://www.analog.com/.

[37] Measurement Specialties Inc., "LDT-052K Piezoelectric Film Sensor," 2004, http://www.msiusa.com/.

[38] T. Martin, M. Jones, J. Edmison, and R. Shenoy, "Towards a design framework for wearable electronic textiles," in *Proceedings of the Seventh International Symposium on Wearable Computing*. ISWC 2003, October 2003, pp. 190–199.

[39] CMU Graphics Lab Motion Capture Database, "http://mocap.cs.cmu.edu/search.html," 2003.

[40] Motion Labs Inc., "C3D.org," 2004, http://www.c3d.org/.

[41] D. A. Winter, *Biomechanics and Motor Control of Human Movement, 2nd Edition*. John Wiley and Sons, 1990.

[42] Unknown, "Simple Pendulum," 2004, http://hyperphysics.phy-astr.gsu.edu/hbase/pend.html.

[43] Mathworks, "MATLAB," 2004, http://www.mathworks.com.

[44] Analog Devices Inc., "Using the ADXL202 in Pedometer and Personal Navigation Applications," 2004.